

1 Use of automatic radiosonde launchers to measure temperature and humidity 2 profiles from the GRUAN perspective

3
4 Fabio Madonna¹, Rigel Kivi², Jean-Charles Dupont³, Bruce Ingleby⁴, Masatomo Fujiwara⁵, Gonzague
5 Romanens⁶, Miguel Hernandez⁷, Xavier Calbet⁷, Marco Rosoldi¹, Aldo Giunta¹, Tomi Karppinen²,
6 Masami Iwabuchi⁸, Shunsuke Hoshino⁹, Christoph von Rohden¹⁰, Peter William Thorne¹¹

7
8 ¹Consiglio Nazionale delle Ricerche - Istituto di Metodologie per l'Analisi Ambientale (CNR-IMAA), Tito Scalo (Potenza), Italy

9 ²Finnish Meteorological Institute, Helsinki, Finland

10 ³Institut Pierre et Simon Laplace (IPSL), Paris, France

11 ⁴European Centre for Medium-range Weather Forecasts (ECWMF), Reading, UK

12 ⁵Hokkaido University, Sapporo, Japan

13 ⁶MeteoSwiss, Payerne, Switzerland

14 ⁷Agencia Estatal de Meteorología, Madrid, Spain

15 ⁸Japan Meteorological Agency (JMA), Tokyo, Japan.

16 ⁹Aerological Observatory, Tsukuba, Ibaraki, Japan.

17 ¹⁰Deutscher Wetterdienst (DWD), GRUAN Lead Centre, Lindenberg, Germany.

18 ¹¹Irish Climate Analysis and Research Units, Dept. of Geography, Maynooth University, Maynooth, Ireland.

19 **Abstract**

20
21 In the last two decades, technological progress has not only seen improvements to the quality of
22 atmospheric upper-air observations, but also provided the opportunity to design and implement
23 automated systems able to replace measurement procedures typically performed manually.
24 Radiosoundings, which remain one of the primary data sources for weather and climate
25 applications, are still largely performed around the world manually, although increasingly fully
26 automated upper-air observations are used, from urban areas to the remotest locations, which
27 minimise operating costs and challenges in performing radiosounding launches. This analysis
28 presents a first step to demonstrating the reliability of the Automatic Radiosonde Launchers (ARLs)
29 provided by Vaisala, Meteomodem and Meisei. The metadata and datasets collected by a few
30 existing ARLs operated by GRUAN certified or candidate sites (Sodankylä , Payerne, Trappes,
31 Potenza) have been investigated and a comparative analysis of the technical performance (i.e.
32 manual vs ARL) is reported. The performance of ARLs is evaluated as being similar or superior to
33 those achieved with the traditional manual launches in terms of percentage of successful launches,
34 balloon burst and ascent speed. For both temperature and relative humidity, the ground check
35 comparisons showed a negative bias of a few tenths of a degree and % RH, respectively. Two
36 datasets of parallel soundings between manual and ARL-based measurements, using identical sonde
37 models, provided by Sodankylä and Faa'a stations showed mean differences between the ARL and
38 manual launches smaller than ± 0.2 K up to 10 hPa for the temperature profiles. For relative
39 humidity, differences were smaller than 1% RH for the Sodankylä dataset up to 300 hPa, while they
40 were smaller than 0.7% RH for Faa'a station. Finally, the observation-minus-background (O-B) mean

41 and rms statistics for German RS92 and RS41 stations which operate a mix of manual and ARL launch
42 protocols, calculated using the ECMWF forecast model, are very similar, although RS41 shows larger
43 rms(O-B) differences for ARL stations, in particular for temperature and wind. A discussion on the
44 potential next steps proposed by GRUAN community and other parties is provided, with the aim to
45 lay the basis for the elaboration of a strategy to fully demonstrate the value of ARLs and guarantee
46 that the provided products are traceable and suitable for the creation of GRUAN data products.

47
48 **1. Introduction**

49 Radiosondes are one of the primary sources of upper-air data for weather and climate monitoring.
50 Despite the advent and the fast integration of GNSS-RO (radio occultation) as an effective source of
51 upper-air temperature data (Ho et al., 2017), radiosondes will likely remain an indispensable source
52 of free-atmosphere observational data into the future. Radiosonde observations are applied to a
53 broad spectrum of applications, being input data for weather prediction models and global
54 reanalysis, nowcasting, pollution and radiative transfer models, monitoring data for weather and
55 climate change research, and ground reference for satellite and also for other in-situ and remote
56 sensing profiling data.

57 The analysis of historical radiosonde data archives has repeatedly highlighted that changes in
58 operational radiosondes introduce clear discontinuities in the collected time series (Thorne et al.,
59 2005; Sherwood et al., 2008; Haimberger et al., 2011). Moreover, where radiosonde observations
60 have been used in numerical weather prediction, systematic errors have sometimes been
61 disregarded and the instrumental uncertainties have been estimated in a non-rigorous way
62 (Carminati et al., 2019). Nowadays, there is a broad consensus on the need to have reference
63 measurements with quantified traceable uncertainties for scientific and user-oriented applications.
64 The GCOS Reference upper-air network (GRUAN) provides fundamental guidelines for establishing
65 and maintaining reference-quality atmospheric observations which are based on principal concepts
66 of metrology, in particular, traceability (Bodeker et al., 2016).

67 Apart from direct instrument performance aspects of the radiosounding equipment and radiosonde
68 model, it must be acknowledged that there are many challenges in performing radiosounding
69 launches. During the preparation and launch phase, many circumstances may interfere with the
70 smooth operation of radiosoundings such as undertaking launches at night, harsh meteorological
71 conditions for balloon train preparation, if any, and safe handling when using hydrogen as balloon
72 gas, and last but not least the risk of errors/mishandling by the operators. Additional expenditure

73 may be required when observations are performed in remote regions of the globe, including the
74 polar regions, deserts, or remote islands.

75 Since the start of radiosounding efforts in the early-to-mid 20th Century, the radiosounding systems
76 and the radiosondes themselves have radically changed in size, weight, and performance. For
77 example, a very important innovation was the automation of the data processing and message
78 production from about 1980. Of particular note is that thanks to new technologies, over recent
79 decades, three manufacturers have developed and deployed fully Automatic Radiosonde Launchers
80 (ARL) able to perform unmanned soundings.

81 ARL are robotic systems able to complete in an automatic fashion almost all of the operations
82 performed manually by an operator during radiosounding launch preparation and release, including
83 the implementation of ground check procedures. The advantages of ARLs are in the reduction of
84 the challenges described above as well as in the reduced running costs of a sounding station (e.g.
85 reduction in the need for trained staff and the trend of automating hydrogen production due to cost
86 reasons and to the helium international crisis) and in ameliorating problems of recruiting long-term
87 operators for remote locations. Nevertheless, it must be also stressed that the system must be
88 regularly stocked and maintained to avoid major issues and high repair costs being incurred. In
89 addition, with changes in the radiosonde technology, updates of the systems might be required to
90 enable the use of a new radiosonde type, with periodical costs (variable, every 3-6 years) which
91 might be substantial for a station. In 2018, NOAA-NCEI published stories on its website which show
92 the potential benefits of using ARLs ([http://www.noaa.gov/stories/up-up-and-away-6-benefits-of-
93 automated-weather-balloon-launches](http://www.noaa.gov/stories/up-up-and-away-6-benefits-of-automated-weather-balloon-launches)). Within these stories as well as from the feedback collected
94 within the GRUAN community, several radiosonde stations have reported benefits from the use of
95 ARL and an increase in the percentage of successful soundings with a potential reduction of missing
96 data in the collected data records.

97 Using recent ECMWF statistics on the number of stations transmitting data to the WMO Information
98 System (WIS) and information provided by the GRUAN community and others, there are about 90
99 ARLs (Figure 1) providing data versus about 700 manual stations. ARL stations cover many countries
100 and remote regions, including Arctic and Antarctic locations as well as a broad suite of remote Pacific
101 and other island locations. As far as is known many of the ARL stations only make automated
102 launches. In addition, there are a few more stations, used by research institutions or environmental
103 agencies, not transmitting data via the Global Telecommunication System (GTS) of the WMO

104 Information System (WIS). The total number of stations operating an ARL worldwide has increased
105 within the last decade (see Table A1 and A2 in Appendix A).

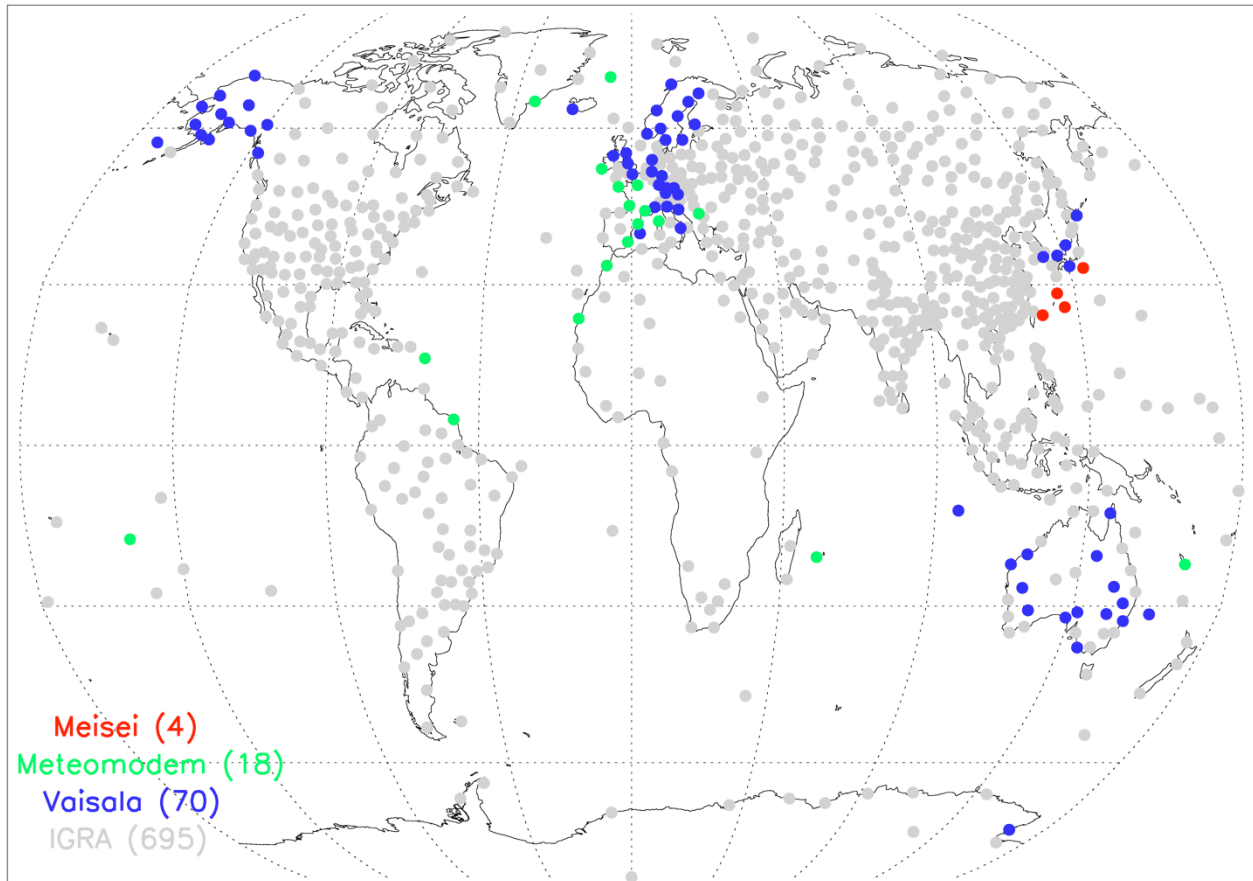
106 Vaisala introduced its first automatic system in 1990, Meisei in 2006 and Meteomodem in 2009.
107 Despite their relatively recent development and deployment, ARLs appear to be successful, and the
108 number of deployed systems will likely increase in the future. However, to date there are very few
109 peer-reviewed papers in the literature dealing with ARLs or comparing ARL vs manual data (often
110 limited to specific examples, e.g. Madonna et al., 2011). More specifically, there is currently no side-
111 by-side assessment of quality in comparison to manually launched sondes. The aim of this paper is
112 thus to quantify the reliability and stability of ARLs and assess the accuracy of their data compared
113 to the traditional manual systems. A discussion on the measurement traceability and on the
114 feasibility to use ARLs in a regular way in the GCOS Reference Upper Air Network (www.gruan.org)
115 is also provided. At present, traceability to SI standards is quantified at several GRUAN sites by the
116 use of a Standard Humidity Chamber (SHC) which can be used for ARL before the launcher loading
117 only. The SHC is a simple ventilated chamber ($\sim 4 - 5$ m/s) using distilled water which, during the
118 ground check procedure, is first heated a few degrees above ambient temperature and then cooled
119 to saturate air at 100% relative humidity. The SHC allows a check of each radiosonde at 100% RH
120 using distilled water (or other RH values using solutions with specific salts although these are
121 generally only used at the GRUAN Lead Centre and for sonde characterisation and not operational
122 sounding preparation purposes).

123 The comparison reported in this paper focuses exclusively on temperature and relative humidity
124 profiles and relies upon manufacturer's products (i.e. GRUAN Data Processing based on the raw
125 data collected by the sonde, described in Dirksen et al., 2014, and Kobayashi et al., 2019, is not
126 used).

127 The remainder of the paper is structured as follows. In section 2, a short description of the three
128 ARLs is provided. In section 3, the technical performance of the ARLs is investigated on the basis of
129 statistics comparing the technical efficiency of the ARLs versus the manual sounding stations as well
130 as reporting an analysis of the feedback from station operators collected at the GRUAN sites on the
131 advantages, limitations and technical issues faced to maintain and ensure continuity of ARL
132 operations. Section 4 reports on the effect of the usage of ARLs on the stability and the accuracy of
133 ground-check calibration procedures. Section 5 provides statistics obtained from parallel soundings
134 at different sites for both temperature and humidity profiles. Section 6 discusses the comparison
135 between observation-minus-background (O-B) statistics obtained from ARL data and manually

136 launched data, respectively, using the ECMWF short-range forecast fields. Finally, section 7 provides
137 a summary and a description of the experiments which might be performed to design future ARL
138 setup to enable full measurement system traceability to SI units and, therefore, to meet GRUAN
139 requirements for long term reference climate data.

140



141

142 Figure 1: Map of stations running an Automatic Radiosonde Launcher (ARL) and transmitting the data to the WIS in late
143 2019 (see also Appendix A). Blue dots are the Vaisala ARL, green the Meteomodem, and red the Meisei. In light grey,
144 the manual stations providing data to the WIS in September are also reported. Number of stations for each color is
145 reported in brackets.

146

147 2. Description of existing ARL systems

148

149 2.1 Vaisala Autosonde: brief history and recent system configurations

150 Automation of upper-air sounding data processing has made steady progress since the early 1970's
151 and is now widespread (Kostamo, P., 1992). The Vaisala Autosonde project was started in late 1992
152 and a working prototype presented at CIMO, Vienna, in 1993. The prototype was tested in Norway
153 and Sweden in 1993 and 1994. This coincided with the replacement of manual balloon tracking

154 systems by Omega and Loran networks. It was provided by Vaisala Oy (Finland) and was
155 permanently installed at the Landvetter station in Sweden in 1994. As of today, about 80 Vaisala
156 ARLs have been installed worldwide and the number of soundings performed has exceeded
157 800,000, while the annual number of new soundings will soon exceed 70,000 (Lilja et al., 2018).
158 With the newest Autosonde model it is possible to perform 60 soundings without replenishment,
159 while the earlier models allowed up to 24 soundings.

160 The first radiosonde type used for an automatic launch was the RS80-15N (during 1994-2006). The
161 RS80 radiosonde was followed by the models RS92 (manufactured 2005-2017) and then RS41
162 (available since late 2013). The RS92 radiosonde (Dirksen et al. 2014) performs measurements with
163 a nominal measurement uncertainty (provided by the manufacturer) of 0.5°C for temperature, 1.0
164 hPa for pressure below 100 hPa and 0.6 hPa above, 0.15 m s⁻¹ for wind speed and 5 % RH for relative
165 humidity ([https://www.vaisala.com/sites/default/files/documents/RS92SGP-Datasheet-
166 B210358EN-F-LOW.pdf](https://www.vaisala.com/sites/default/files/documents/RS92SGP-Datasheet-B210358EN-F-LOW.pdf)). RS41 sonde specifications for nominal measurement uncertainties
167 (provided by the manufacturer) are 0.3°C for temperatures below 16 km and 0.4°C above, 0.01 hPa
168 for pressure sensor, 0.15 m s⁻¹ for wind speed and 4 % RH for relative humidity
169 (<https://www.vaisala.com/sites/default/files/documents/RS41-SGP-Datasheet-B211444EN.pdf>).

170 Note that the Vaisala RS41 radiosondes are of two different types: RS41-SG which are not equipped
171 with a pressure sensor and using the GNSS-based method to infer pressure (Lehtinen, 2014), and
172 RS41-SGP which uses a pressure sensor as the default. More stations use the RS41-SGP than the
173 RS41-SG: in November 2019, 158 stations type were using RS41-SGP versus 66 stations using type
174 RS41-SG.

175 To launch the RS41 sondes, the Autosonde Ground Check (GC) procedure has been updated. The
176 GC device of the RS41 sondes consists of a wall-mounted box and an activator that contains a
177 wireless reader for the radiosonde. The device is designed to automatically activate the radiosonde
178 and to enable wireless data transfer. An activator is connected to the reader box with a coaxial
179 cable. The ground check device also includes a barometer while the surface pressure used as a
180 reference for the launch is obtained from a separate co-located automatic weather station.
181 However, the ground check pressure device can be used as a backup for the weather station sensor.
182 The GC performs a temperature check where the actual temperature sensor is compared with the
183 one integrated on the humidity sensor chip. In contrast to the RS92 GC, a pre-flight fine-tuning of
184 the temperature measurement is no longer applied to the RS41 because the manufacturer found

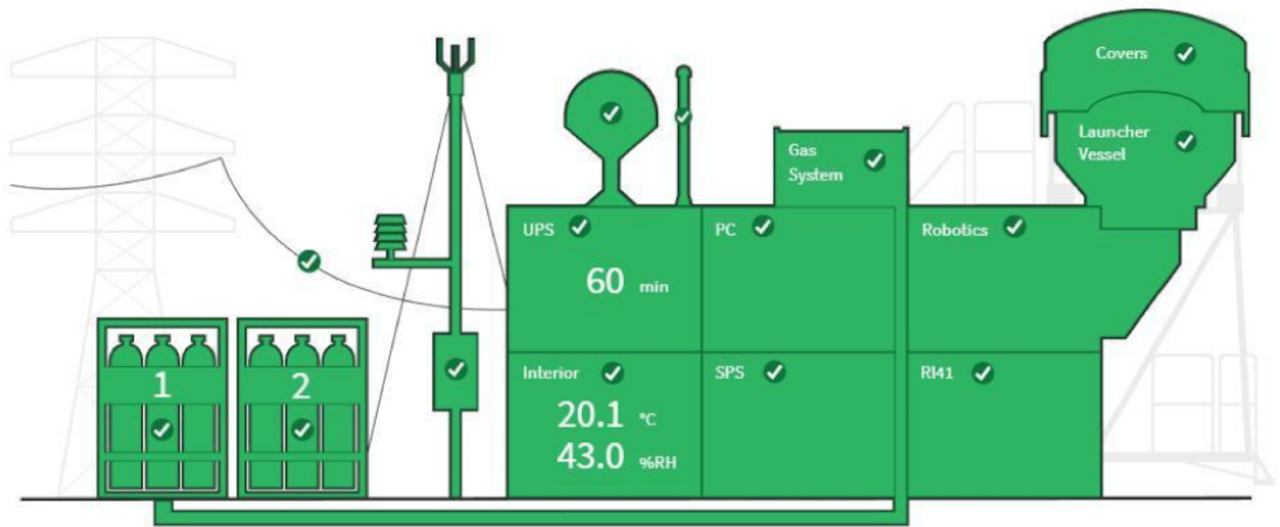
185 that the performance of the RS41 temperature measurement is practically unchanged during
186 storage.

187 Humidity is also checked in the GC. The RS41 humidity check consists of two main steps – the sensor
188 reconditioning phase and the 0% RH check. In the reconditioning phase, the sensor is heated to
189 remove possible contaminants that might affect the measurement results and cause a slight
190 degradation of the sensitivity of the humidity sensor. Then, the humidity sensor is checked and then
191 corrected against a dry humidity condition. Specifically, the dry reference condition of the new zero
192 humidity check is generated in open air by heating the sensor using the integrated heating element
193 on the sensor chip. The procedure is based on the decrease of relative humidity towards zero as the
194 temperature rises high enough (Vaisala, 2013; Vaisala 2015). This method differs from the RS92 GC
195 where the correction was based on a dry condition generated with desiccants, whose drying
196 capacity gradually fades with time.

197 The radiosonde's humidity sensor is reconditioned and ground check performed during the
198 automated launch preparation in order to ensure similar performance as in manual stations (Lilja et
199 al., 2018). The top panel of Figure 2 provides a schematic picture of the most recent VAISALA AS41
200 Autosonde system configuration while the bottom panel shows a photograph of the Autosonde
201 system operational at the Finnish Meteorological Institute GRUAN site in Sodankylä (WIGOS station
202 identifier=0-20000-0-02836, 67.34 °N, 26.63 °E, 179 m a.s.l.). In Table 1, the basic technical data of
203 the Autosonde AS41 are reported. More details on the specifications of the Vaisala Autosonde AS41
204 can be found in the datasheet (B211636EN-A_2 pages.pdf, last accessed September 20, 2019)
205 available on the Vaisala website (<https://www.vaisala.com>).

206

207



208

209

210 Figure 2: Schematics of the VAISALA Autosonde AS41 system in its most recent configuration (top panel), and photo of
 211 the Autosonde system AS15 (bottom panel) operational at the Finnish Meteorological Institute GRUAN site in Sodankylä
 212 (WIGOS station identifier=0-20000-0-02836, 67.34 °N, 26.63 °E, 179 m a.s.l., see Vaisala 2018,
 213 [https://www.vaisala.com/sites/default/files/documents/AUTOSONDE%20AS41%20Datasheet%20B211636EN-
 214 A_2%20pages.pdf](https://www.vaisala.com/sites/default/files/documents/AUTOSONDE%20AS41%20Datasheet%20B211636EN-A_2%20pages.pdf))).

215

216

217

218

219

Table 1: Autosonde AS41 technical data (Vaisala, 2018)

Dimensions	Width: 3.30 m
	Length: 7.80 m
Launch Tube Diameter	2.20 m
Height during transport	2.90 m
Total height with launcher tube	5.10 m
Gross weight with launcher tube	7.5 t
Electrical energy consumption	< 1 kW (without air conditioning)

220

221

222 2.2 Meteomodem Robotsonde

223 The Meteomodem ARL is an automatic balloon launcher system that can perform up to 12 or 24
 224 soundings without any manual control (<http://www.Meteomodem.com/docs/en/Leaflet-robotsonde.pdf>). The system is compatible with M10 and M20 Meteomodem radiosonde types. It
 225 is built in a robust dry maritime container and composed of the following subsystems (Figure 3):
 226

- 227 ● Operator room with electronic control unit and PC workstation, isolated from the launch tube
 228 by an air-tight safety door, and used only during radiosonde setup and restocking;
- 229 ● Carrousel with 12 or 24 removable containers for balloon trains, and with individual flexible
 230 cover on balloon locations which preserve balloons from desiccation;
- 231 ● Launch tube for balloon inflation and release and pneumatic equipment or pressurized air
 232 network;
- 233 ● Optionally, a double-door entrance to protect from strong winds, rain, drifting snow or
 234 sandstorms.

235 The Meteomodem ARL main specifications are reported in Table 2. Worldwide there are 19
 236 Meteomodem ARL systems automatically launching Meteomodem M10 radiosondes. The
 237 specifications for nominal measurement uncertainties (provided by the manufacturer) are 0.58°C
 238 for temperature, 1 hPa for pressure, 0.15 m s⁻¹ for wind speed and 5 % RH for relative humidity
 239 (www.Meteomodem.com/docs/en/Leaflet-m10.pdf).

240

241

Table 2: Meteomodem ARL specifications

Dimensions	Width: 2.44 m
	Length: 6.00 m
Launch Tube Diameter	2.00 m
Height during transport	3.10 m
Total height with launcher tube	3.60 m
Gross weight with launcher tube	3.5 t
Electrical energy consumption	< 1 kW (without air conditioning)

242

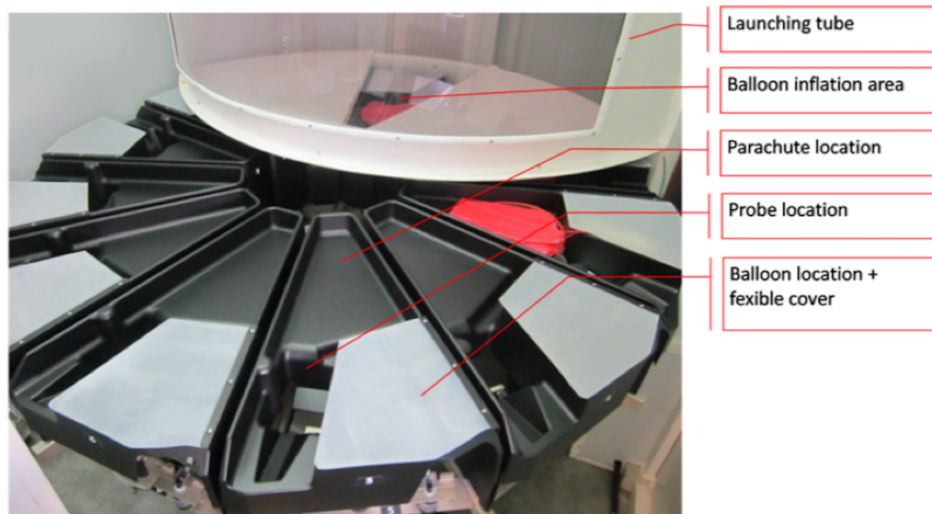
243

244 For each launch, there is a preparation phase which comprises the radiosonde GC and the loading
245 of the balloon train (with the radiosonde, the unwinder, the parachute, and the balloon) into
246 individual bins before finally sounding parameters (e.g. launch time schedule, inflation volume, etc.)
247 are setup.

248 During the launch phase, before powering on the sonde, the system performs a scan of the
249 bandwidth in order to detect possible radio interference, then the radiosonde battery pack is
250 powered on through an infrared link. According to the scan result, the system sets up the new
251 frequency through an infrared link, and GNSS signal collection is initialized. Then, the system loads
252 the calibration data of the relevant radiosonde stored during the preparation phase and checks
253 consistency with PTU criteria. The Meteomodem ARL GC is a standard Meteomodem GC which
254 consists of a sealed box enclosing a reference and a fan which homogenises the inside temperature
255 and relative humidity. It is recommended to return the Meteomodem GC every 3 years for
256 calibration. The calibration is made with a certified Rotronic HC2A-S probe
257 (<https://www.rotronic.com/en/hc2a-s.html>).

258 Then, the ARL records the ground check data and the metadata. Balloon inflation starts accordingly:
259 the system monitors a flowmeter to inflate the balloon to the specified volume. The ARL may use
260 either helium or hydrogen gas. Finally, the balloon is released at the specified launch time. In case
261 of launch failure before balloon release or during the flight, the procedure will restart for a new
262 sounding immediately or can alternatively be manually launched according to a preset time
263 schedule. At any time, an immediate start of the launch procedure can be initiated by an operator
264 (locally or remotely).

265
266



267
268
269
270
271
272

Figure 3: Meteomodem Robotsonde (top panel) launching a balloon at Trappes station (WIGOS station identifier=0-20000-0-07145, 48.77N, 2.01E, 168 m asl, <http://www.Meteomodem.com/robotsonde.html>) and photograph of the carousel of Meteomodem Robotsonde with the balloon location (bottom panel).

273 For those stations operating an ARL and adopting a protocol based on GRUAN recommendations
274 (Dirksen et al., 2014), as at Trappes station (WIGOS station identifier=0-20000-0-07145, 48.77N,
275 2.02E, 168 m asl, top panel of Figure 2.2), the GRUAN M10 ground check procedure is performed in
276 two steps: 5 minutes in a ventilated hut in ambient conditions together with calibrated T and RH
277 sensors and, further, another 5 minutes to test the radiosonde performance in the SHC. Then each
278 radiosonde is loaded in the ARL carousel (bottom panel of Figure 3).

279 A technical document describing the M10 sensor, corrections and uncertainties for both the
280 temperature and relative humidity sensors will become available through the GRUAN community
281 as soon as a Meteomodem M10 GRUAN data product is available.

282

283 **2.3 Meisei Automated Radiosonde System**

284 The Meisei ARL, named “Automated Radiosonde System” is designed for fail-safe operation and
285 high remote operability. Compared to the previous version developed in 2006, the new system, still
286 under improvement, is able to load more radiosondes thanks to the development of the Meisei
287 “Canister Type”. The operator can preload a maximum number of 40 sondes in the so-called
288 "Canister modules". The canister has been recently implemented to reduce failures. Once the
289 launch procedure has started, the respective canister fills a balloon independently. The right
290 canister module and the left canister module are independent systems. It realizes high observation
291 continuity by duplicating gas, air and electric systems. The canister module on one side can be
292 moved to the preparation room to load the sonde and facilitate the operator’s work. The new ARL
293 version can also recover from balloon bursts without human intervention at the site by using a
294 balloon from another canister. In the previous version, an operator had to visit the ARL to remove
295 broken balloons and restart the ARL during the observation window in such cases.

296 The new system is also equipped with a new simplified wind shield for launches in strong wind
297 conditions. All information and data are stored in a database available for each ARL. Various central
298 monitoring/control functions are provided by using application software and a web browser to
299 access the database on the workstation installed in the ARL. The Meisei ARL GC consists of a
300 temperature and humidity reference sensor and an inspection box. The GC is performed before the
301 sonde loading. The results from the GC are not used in the data processing but only to check if there
302 are anomalies in the radiosondes.

303 In Table 3, the Meisei Automated Radiosonde System specifications are provided. Figure 4 shows a
304 photo of the system along with a sketch of the internals of system container. For more details on
305 the Meisei ARL experimental setup visit the Meisei website (<http://www.meisei.jp/ars>). Japan
306 Meteorological Agency (JMA) has used Meisei ARLs data since 2006. Parallel radiosoundings of auto
307 launch and manual launch have not been done yet. This is the reason why this paper does not show
308 additional datasets or comparisons involving Meisei ARL; therefore, the description of the Meisei
309 ARL is the only information which can be shared with readers, according to recommendations
310 provided by Meisei.

311

312

Table 3: Meisei ARS specifications

Dimensions	Width: 2.50 m
	Length: 6.20 m
Launch Tube Diameter	2.20 m x 1.80 m square
Height during transport	3.10 m
Total height with launcher tube	1.90 m (2.80 m including windshield)
Gross weight with launcher tube	6 t
Electrical energy consumption	< 1 kW (without air conditioning)

313

314

315 3. Technical performance

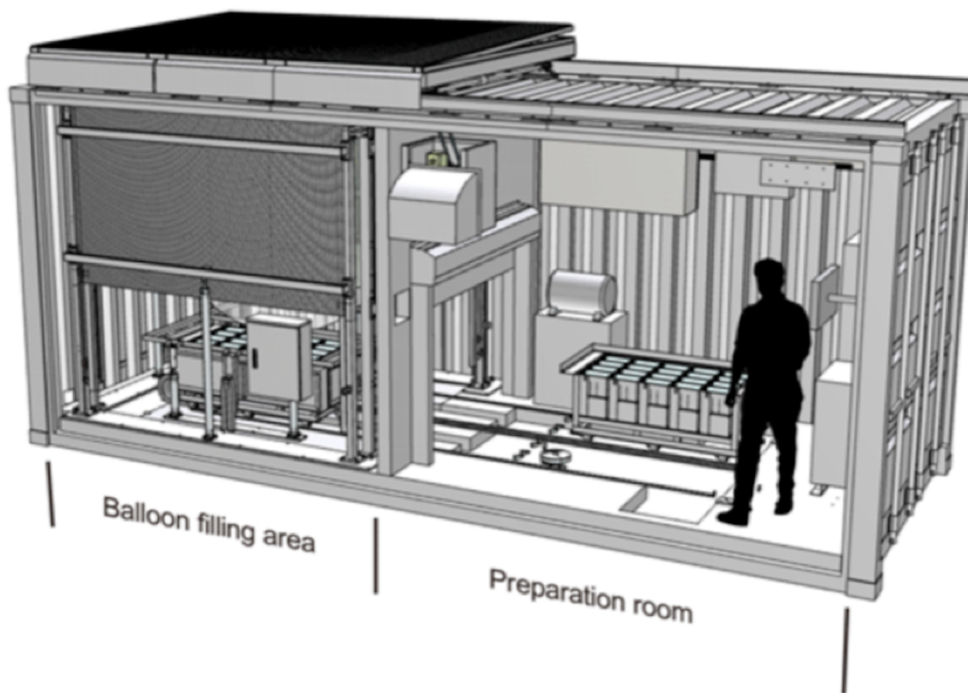
316

317 Beyond the automation of the radiosonde launch procedure, there are two main differences
318 between an ARL and a manual launch:

- 319 ● Ground check procedures may be performed only during the sonde loading in the carousel
320 chamber, days or weeks before the sonde launch, though there is a trend towards less
321 frequent stocking;
- 322 ● The use of independent and traceable calibration standards like the Standard Humidity
323 Chamber (SHC) is possible but only before the launcher loading (also in this case one or more
324 days before the launch).

325 Both these aspects will be discussed in the following sections which provide potential technical
326 solutions to address the gaps between manual and automatic launch procedures in terms of
327 performance and traceability.

328



329

330 Figure 4: Picture of a Meisei Automatic Balloon Launcher (top panel) and sketch of the internals of ARL container in its
331 most updated configuration (bottom panel).

332

333 This section aims to provide a classification of the main challenges met by the stations which have
334 operated ARLs over several years and to assess the technical performance of the ARLs compared to
335 manual launches. The section is built upon the feedback provided by the GRUAN sites in response
336 to a survey for the collection of ARL information. Most of the ARLs at GRUAN sites are from Vaisala
337 (thus the analysis is not representative of Meisei and Meteomodem systems due to the very limited
338 feedback available for these systems). Given the small sample size, this is presented qualitatively

339 rather than quantitatively and it is anonymised. Examples of technical performance in the field are
340 then provided for a Vaisala and a Meteomodem ARL operating the most recent updated version of
341 the respective manufactured systems (at Payerne and Trappes stations).

342 A conceptual diagram to represent a generic ARL is provided in Figure 5: each ARL can be
343 schematically divided into 4 areas as follows:

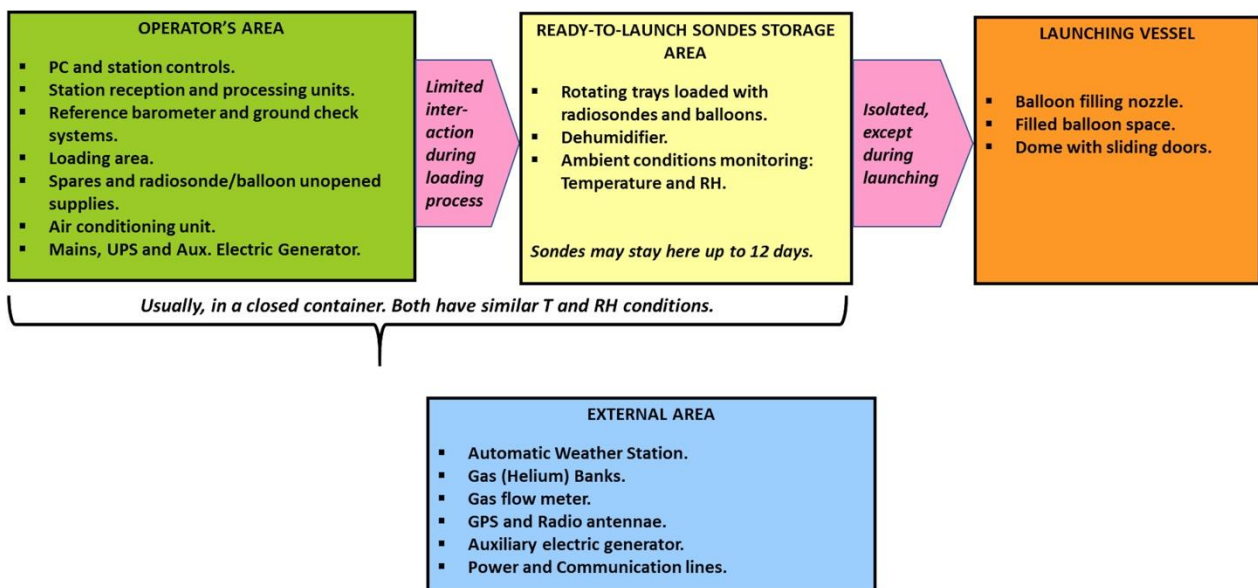
- 344 ● the operator's area, where the operators can manage the system, prepare radiosondes and
345 balloons to be uploaded and where the station reception and processing units are located;
- 346 ● the ready-to-launch sondes storage area, built around the ARL rotating trays, where most
347 of the automated technologies are implemented to allow a completely unmanned launch;
- 348 ● the launching vessel area, where the balloon is filled and becomes ready for the launch;
- 349 ● external area, where all the ancillary instruments, such as the weather station and GNSS
350 antenna, are located along with gas tanks.

351 For each area, the weakest points identified from the GRUAN sites operating an ARL are:

- 352 ● in the operator's area, most of the issues are related to the not infrequent failure of power
353 supply system or of the air conditioning system, often related to a major failure of the power
354 supply at the measurement station itself. This represents a particular weakness in the use
355 of ARLs in remote areas where power supply is generally less stable, and where logically the
356 ARL might be an obvious choice. A few sites also reported issues in the software and logic
357 controllers;
- 358 ● the ready-to-launch sonde storage area is assessed as the most efficient part of ARLs, where
359 few issues reported. The most critical issue identified in this area is the infrequent failure of
360 the air compressor;
- 361 ● the launching vessel area is where the balloon is filled and launched and where, therefore,
362 we have a high exposure to many environmental factors like harsh climate, dust, animals,
363 etc., which can strongly affect a successful launch also with later effects to the balloon and
364 early burst. Several issues were raised by the stations related to challenges in the balloon
365 inflation process, failure of balloon presence sensor allowing launch of under-inflated
366 balloons, gas tubes bent and frozen gas hoses, balloon blocked on the tray, failure of the
367 rams which open vessel cover doors (this concerns Vaisala or Meisei, and not Meteomodem
368 ARL). Other issues noted were delays in launch detection time compared to the actual
369 launch time, and occasional break of the radiosonde string at launch (for Meisei);

- the external area, is another critical area where several problems have been reported about the gas flow meter and the switching between the gas tanks (one close to empty and the other fully filled). Extreme weather conditions (e.g. very strong winds) can make the launch more difficult, despite the additional screens protecting the balloon flight in the first 2-3 meters above the ARL (only for Vaisala and Meisei).

The problems listed above are not common to all the ARLs, each system has its own specific issues. While the feedback reported from GRUAN stations can provide a first assessment of the challenges in operating an ARL, this study cannot assess challenges in the operation of each specific model and it cannot quantify the improvements of each ARL with the time. The issues discussed above could be used as recommendations to the manufacturers to foster further improvements of the systems. The ARLs are typically maintained by the manufacturers on an annual check up (performed remotely) and major maintenance approximately every 3 years. This maintenance schedule, if applied at each station can increase the reliability of the systems over both the short- and long-term, although it generates additional costs.



385
386
387 Figure 5: Conceptual diagram of a typical automatic radiosonde launcher divided in four main areas: operator's area (green), ready-to-launch sondes storage area (yellow), launching vessel area (orange) and external area (cyan).
388
389

390 To assess the effective technical performances of the ARL launches vs manual launches, in Table 4
391 and 5, examples of the statistics collected at two GRUAN sites running an ARL, Payerne (WIGOS
392 station identifier=0-20000-0-06610, 46.82N, 6.93E, 490m asl), operated by MeteoSwiss, and
393 Trappes, operated by Meteo France, respectively, are reported. The Table provides a summary of

394 pertinent characteristics of the ARL versus manual launches. For Payerne, statistics are related only
395 to the automatic and manual launches performed since April 2018 (on average, ARL nine per week,
396 manual five per week) using the Vaisala AS15 ARL. For Trappes, manual launches were performed
397 in the period 2012-2014, while the Meteomodem Robotsonde has been operated in the period
398 2016-2018; in both cases two launches per day were performed with similar daily scheduling.
399 At Payerne, since April 2018 the Vaisala ARL has realized 470 successful flights per year, according
400 to MeteoSwiss standards¹, while manual launches have been 260 per year. Despite the use of
401 different balloon sizes due to the fact that for manual launches bigger balloons are often used to
402 perform ozonesoundings, the percentage of successful launches as well the percentage of sondes
403 reaching 10 hPa pressure level is indistinguishable between the ARL and the manual launches, with
404 a limited use of spare sondes due to the failure of scheduled launches for the ARL (4 %). Ascent
405 speed statistics are very close with better performance of the ARL in preventing very low balloon
406 gas filling and thus slow ascents.

407 At Trappes station (Table 5), during the period January 2016 to December 2018, the Meteomodem
408 ARL Robotsonde has carried out 1908 successful flights, according to MeteoFrance standards², out
409 of a total of 1956. For each of the remaining 48 flights, a spare automatic launch was performed
410 which fulfilled the requirements of MeteoFrance. The mean percentage of successful launches is
411 97.9% (2016: 95.5%, 2017: 98.2%, 2018: 99.1%, 2019(Jan-Oct): 98.6%, see Figure 6) with an evident
412 improvement using ARL in the percentage of sondes reaching 10 hPa pressure level (80%) compared
413 to the manual launches (60 %). The use of Totex balloons is one of the reasons for the improvement
414 and further improvement was achieved by increasing the size of the balloon. Moreover, since
415 November 2016 Meteomodem has installed a flexible cover which assures that during the storage
416 the balloon is less exposed to contact with the air-conditioned environment. This seems to reduce
417 the effects of drier air on the balloon and improve its performance in terms of burst altitude
418 (standard deviation of burst altitude is reduced after the installation of the cover – not shown). For
419 the balloon ascent speed, comparison statistics between ARL and manual launches show also similar
420 results. According to the information shared by Meteomodem, it is also possible to add that,
421 compared to all the ARLs operated at other sites during the same period reported in Table 5, the

¹ According to MeteoSwiss, a “successful flight” is a launch with a balloon burst at a pressure lower than 100 hPa, with no telemetry lost or sensor failure.

² According to MeteoFrance, a “successful flight” is a launch with a balloon burst at a pressure lower than 150 hPa, with no telemetry lost or sensor failure.

422 Trappes ARL has typically similar failure statistics. The time evolution of the failure (Figure 6) shows
 423 that the number of spares and the number of failures by type halved in three years to reach less
 424 than 2% relative to the number of successful flights. For the 716 flights performed during 2018, the
 425 absolute number of failures is 2 for the ARL (which was a radio loss and an inflation problem), 1
 426 failure due to sensor break, no failure from the software, 1 failure which is not classified by their
 427 automated failure identification and 1 failure due to the use of ARL which can be an operator stop
 428 or an obstructed inflation tube.

429
 430 Table 4: Technical performance of automatic vs manual launches performed at Payerne station
 431 during 2018 for a Vaisala AS15 ARL. Metadata related to the sonde and balloon types are shown
 432 alongside the percentage of success for the launches performed during the reported period, the
 433 percentage of spare sondes used, the balloons bursting before reaching 10 hPa, and the maximum,
 434 minimum and average ascent speed.

435

Station	Automatic	Manual
Station type	AS15	MW41
RS type	RS41	RS41 (+ ECC ozonesonde)
Balloon type	Totex	Totex
Balloon size	800g	800g/1200g/2000g/3000g
Number of launches	470/year	260/year
Percentage of successful flights ³	>99%	>99%
Percentage of spare	4%(spare if P>100hPa)	N/A
Sondes above 10 hPa	92% (based on 2018)	92% (based on 2018)
Max. Ascent speed	6.1 m/s	6 m/s
Min. Ascent speed	3.5 m/s	3 m/s
Avg. Ascent speed	5.2m/s	5m/s

³ Percentage of successful flights out of successful launches.

436
437
438
439

Table 5: Same as Table 4 for Trappes site in the period 2016-2018 and 2012-2014, respectively for a Meteomodem ARL.

Station	Automatic	Manual
Station type	Robotsonde (14/04/2015 to 12/2018)	SR10 (01/01/2012 to 14/04/2015)
RStype	M10	M10
Balloon type	Totex	Hwoyee
Balloon size	350g/1000g	Hwoyee 600g
Number of launches	2106	2113
Percentage of successful flights	99% (based on 2018)	>99% (based on 2012)
Percentage of spare	5% (based on 2018)	N/A
Sondes above 10 hPa	80%	60%
Max. Ascent speed	6 m/s	6 m/s
Min. Ascent speed	4 m/s	4 m/s
Avg. Ascent speed	5 m/s	5.4 m/s

440

441

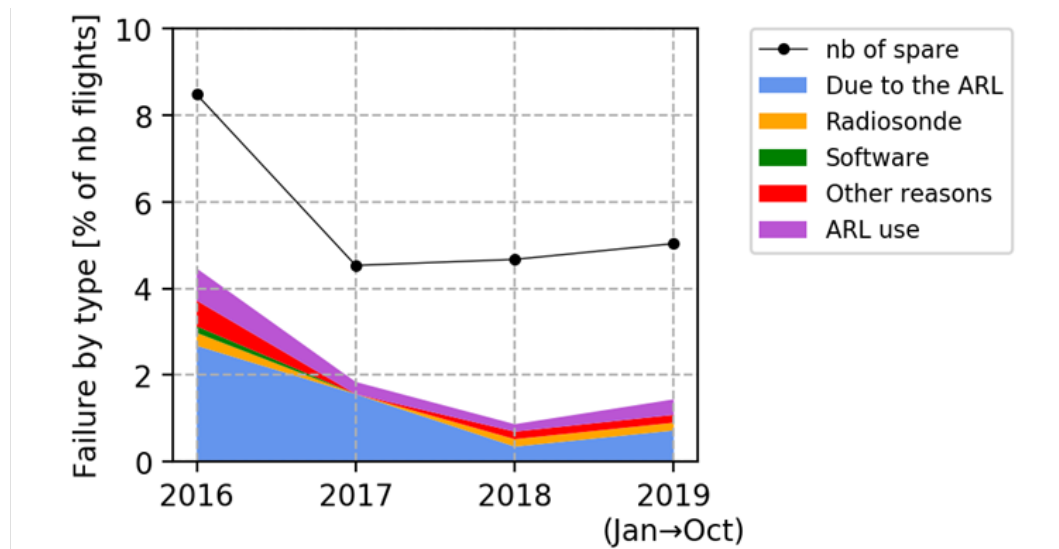
442 It is worthwhile to add that ECMWF noted in some reports that some stations using Meteomodem
443 Robotsondes had anomalously dry, and sometimes warm, values just above the surface relative to
444 the background field. In cool, moist atmospheric conditions the anomalies can be two or three
445 degrees for temperature and larger for dew point temperature. "For technical reasons the launcher
446 has to be kept warm and dry internally, which means that the humidity sensor is initially reading
447 quite low and a bubble of warm/dry air escapes with the balloon at launch - the net effect is that
448 the first few decametres the dewpoint reading is too low." (Ray McGrath, pers. comm. 2015). The
449 issue described above does not affect the profile at higher levels. A similar issue has also been
450 reported for data taken during the first few seconds with Meisei ARL and this is suspected to be due
451 again to the influence of the air inside the launcher.

452 The Meteomodem has recently implemented a new software, EOSCAN, not yet implemented at all
453 the stations, which improves the ARL dataset quality with a number of corrections such as:

454 1. Eliminating the GPS disturbances at the end of the tube that can persist in the first 20 seconds
455 after the release;

456 2. Adjusting for the systematic bias introduced by the fact that the ARL Meteomodem is air
457 conditioned and affecting the first 150 m of the radiosounding profiles.

458



459

460 Figure 6: Cause of failure for the Meteomodem ARL in Trappes as a function of time since the
461 installation date. The black dots are the values of the number (nb) of spare used after the launch
462 failure.

463

4. Stability, ground calibration

464

4.1. Performance of the Vaisala ARL

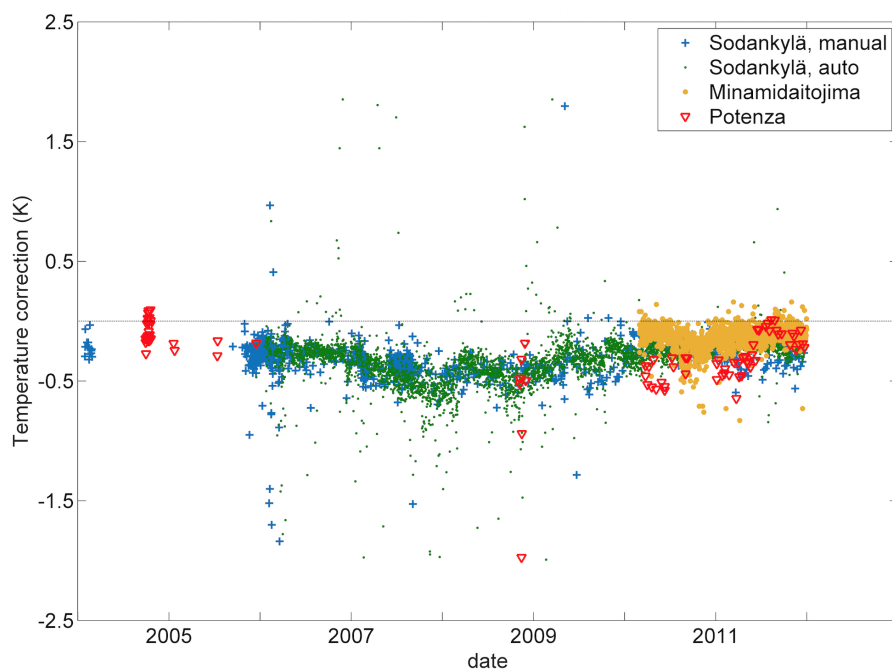
465

466 The performance of the Vaisala ARL has been evaluated through the analysis of a dataset collected
467 at Sodankylä station. The Sodankylä Vaisala ARL was used to regularly launch RS92 radiosondes at
468 11:30 and 23:30 UTC over 2006 to 2012. Manual soundings were periodically performed in parallel
469 using a similar Vaisala DigiCora-3 sounding system throughout this period. Parallel soundings have
470 been selected with launch time difference between 2 minutes and 20 minutes. A total of 283 parallel
471 soundings has been considered: these are distributed evenly across the period, with the exception
472 of 2006, which has more parallel soundings than other years, and most of these are daytime
473 comparisons. In addition, two Vaisala ARL datasets from the Potenza GRUAN station (40.60N,
474 15.72E, 760 m a.s.l.) and the Minamidaitojima station, run by JMA (WIGOS station identifier
475 index=0-20000-0-47945, 25.79N, 131.22E, 15 m a.s.l.), covering a similar time period, though much

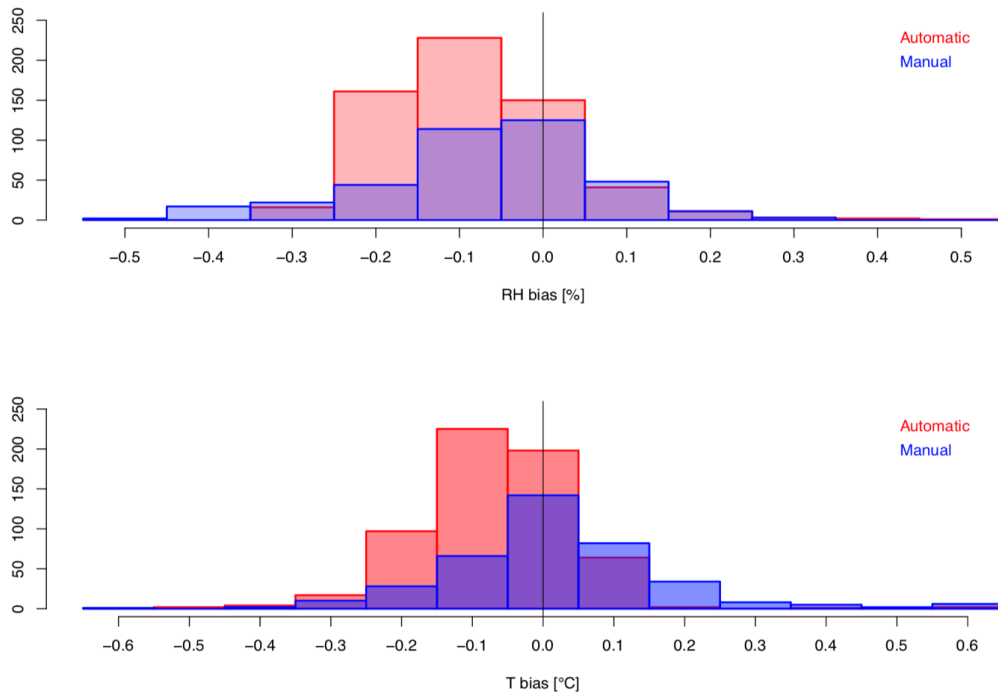
476 smaller sample sizes than in Sodankylä, have been used for comparison. Despite the less intensive
477 sampling, Potenza and Minamidaitojima data are useful data sources to compare with Sodankylä
478 and, specifically, to check consistency of the GC correction across different stations and different
479 batches of Vaisala sondes.

480 The availability of long time series of parallel sounding for the Sodankylä station permits
481 investigation of the system performance also in the pre-launch phase. Two main aspects are
482 evaluated: stability of the ground check correction on temperature, and potential effects related to
483 the time periods the sondes were stored before launch.

484 Figure 7 summarises the temperature correction applied during the GC procedure for the RS92
485 sondes of the above described data sets using the Vaisala GC25 ground check device, with most of
486 the launches performed since 2006. Figure 7 shows similar GC values at Sodankylä, Potenza and
487 Minamidaitojima stations despite the very different locations and launch scheduling, with a
488 negative adjustment of between smaller than -0.5 K before 2010 and smaller than -0.3 K typically
489 applied to most of the RS92 sondes with an improvement of the differences over the time in the
490 batches launched after 2009. The results shown in Figure 7 are based on the assumption that all the
491 reported ARL GC temperature sensors were maintained according to recommendations described
492 in the previous section.



493
494 Figure 7: Time series of the temperature correction (temperature measured by the GC reference sensor minus
495 temperature measured by the sonde) applied during the GC procedure for the RS92 sondes launched at Sodankylä, both
496 manually (blue crosses) and automatically (green dots), and at Minamidaitojima (yellow dots) and Potenza (red
497 triangles, automatically) from 2004 to 2012.



499

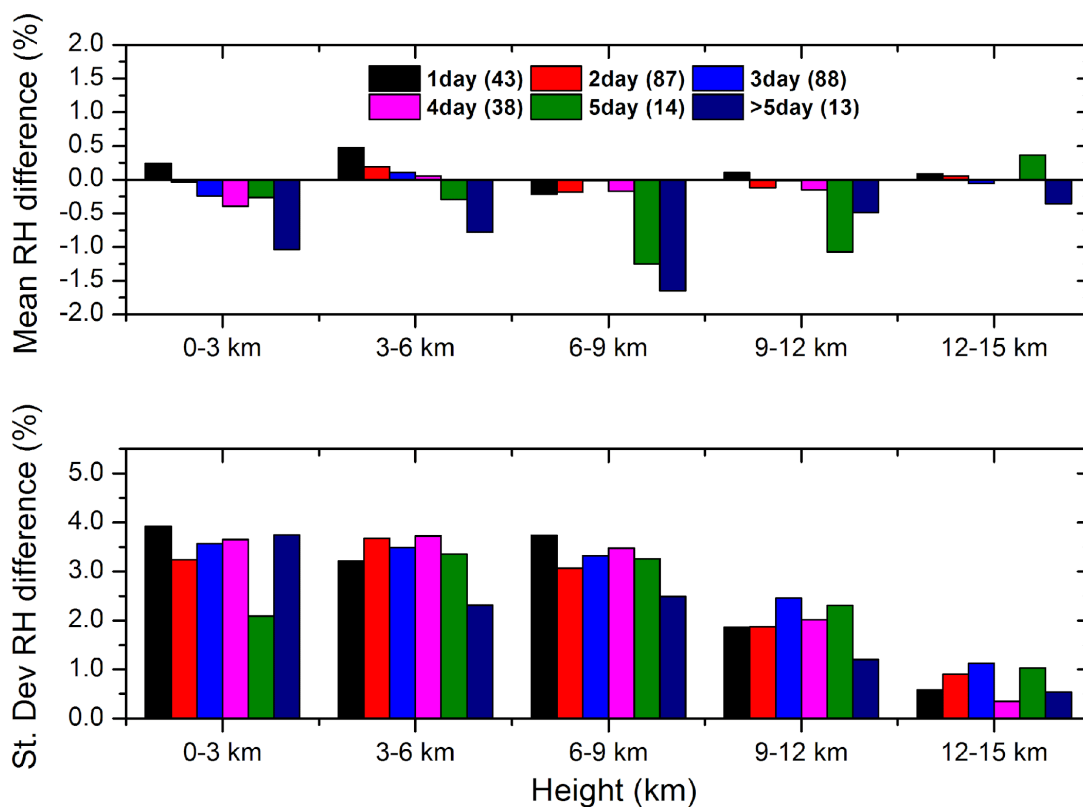
500 Figure 8: Distribution of temperature and relative humidity corrections found during Vaisala GC process for the
 501 automatic and the manual soundings operated at Payerne station using the RS41 radiosonde.
 502

503 Results similar to those from Sodankylä and Potenza GRUAN stations are reported by Payerne
 504 GRUAN station (Figure 8) using the RS41 since April 2018 and operating the Vaisala AS15 ARL. Figure
 505 8 shows that the distribution of temperature and relative humidity corrections have negative
 506 skewness with the GC adjustments within a few tenths of a degree and the average adjustment is
 507 smaller than 0.1 K and 0.1% RH, respectively. These results show an average negative GC corrections
 508 for the ARL in analogy to the results reported above for RS92 sondes at Sodankylä and Potenza,
 509 where also the old Vaisala ARL version was operated. Comparisons with the broader statistics
 510 collected by GRUAN stations launching manually (not shown) reveal results consistent with the GC
 511 time series shown in Figure 7 and 8, thus excluding the presence of clear systematic effects in the
 512 GC corrections due to the use of ARLs. Nevertheless, the small differences observed between the
 513 ARL and manual GC corrections warrant further investigations to understand if performing the GC
 514 in a controlled temperature and humidity environment may generally improve or worsen the
 515 calibration in the long term.

516 In an operational station like Sodankylä, the time between balloon loading and ground check can
 517 vary from day to day. At Sodankylä average loading time was 2-3 days prior to launch for regular
 518 soundings. The ARL software allows also longer times in the tray. Figure 9 shows, at different

519 altitude ranges, the mean differences of simultaneous RH profiles (left panel) measured using the
520 ARL and the manual soundings as a function of the number of days a sonde stays on a tray before
521 launch, from 1 to more than 5 days. The corresponding mean standard deviations are also shown
522 (right panel), while in brackets within the color legend, the number of parallel soundings for each
523 time period is reported. To calculate the statistics shown in section 4 and 5, radiosounding
524 temperature and RH from parallel soundings have been interpolated to a 100-meter vertical grid.
525 Figure 9 shows that there are no RH systematic differences when parallel launches are grouped
526 according to the tray time, except for the launches with a tray time of 5 days or more at altitude
527 levels above 6 km a.g.l., where a mean difference smaller than -2.0 % RH is obtained up to 10-12 km
528 a.g.l. Nevertheless, it must be noted that the size of the sample investigated for these tray time
529 options (5 days and >5 days) is much smaller than for other tray times and these launches include
530 also parallel sounding with longer differences in the respective balloon release time.

531 To test if the estimated RH differences are meaningful, the Wilcoxon Rank Sum Test has been
532 applied. This test is a non-parametric test of the null hypothesis that it is equally likely that a
533 randomly selected value from one population will be less than or greater than a randomly selected
534 value from a second population. If the null hypothesis is rejected, then there is evidence that the
535 medians of the two populations differ. In this study, the Wilcoxon Rank Sum Test has been used
536 instead of the Z-test because of its robustness in case of a small observations sample (i.e. small
537 number of parallel launches) and to avoid assumptions on the underlying data distribution (e.g. data
538 distribution skewed or non-normal). For the RH profiles reported in Figure 9, the probability
539 computed using the Wilcoxon Rank Sum Test ranges within 0.4-0.5 with smaller values only above
540 12 km a.g.l, where the probability becomes greater than 0.2. For the time-in tray classes with a
541 smaller sample of parallel soundings (1 day, 5 day and >5 days), the probability oscillates between
542 0.05 and 0.10. Therefore, it is possible to conclude that we cannot reject the hypothesis that the
543 two data distributions (ARL and manual launches) have the same median value and the reported
544 comparisons are consistent. Finally, the bottom panel of Figure 9 shows that the standard deviations
545 are substantially smaller than 5% RH at all altitude levels without any evident correlation with tray
546 time.

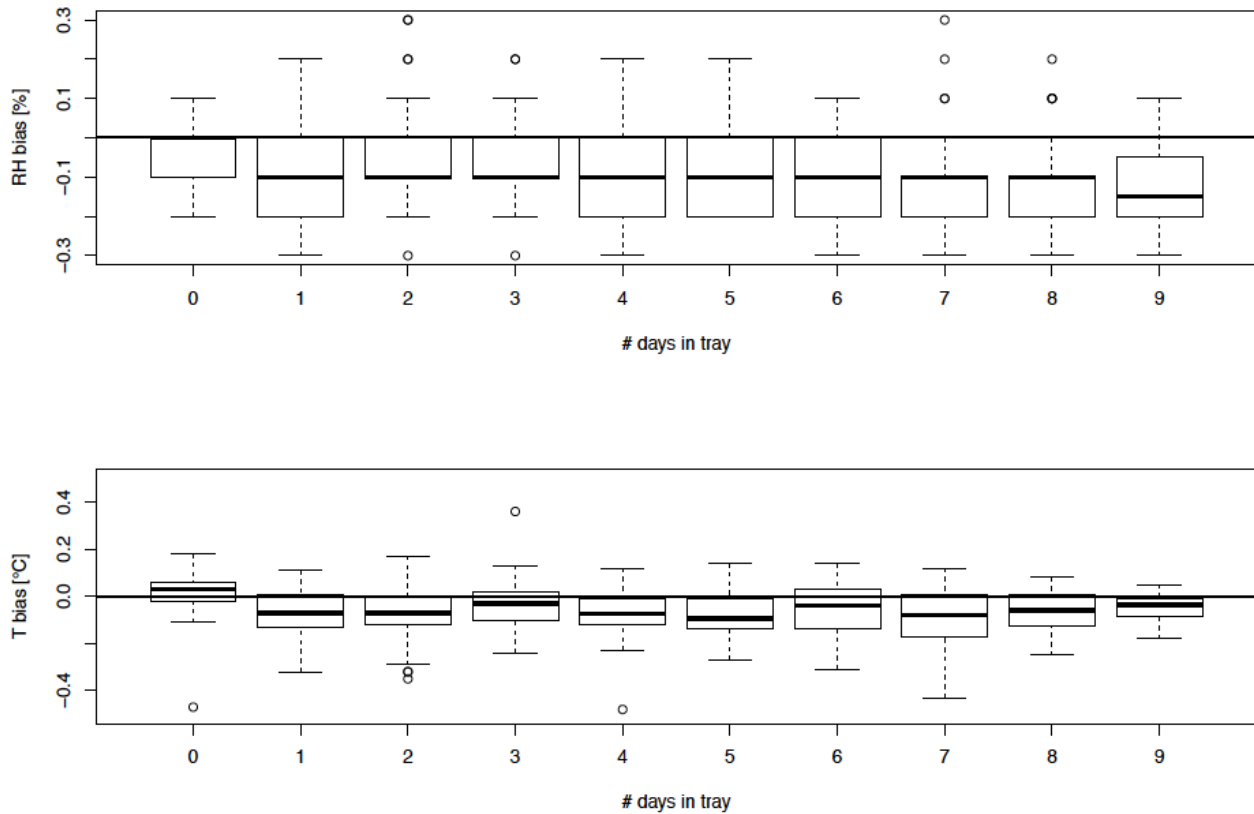


547

548 Figure 9: Mean difference and standard deviation of the RH measured with the manual and automatic system in
 549 Sodankylä at different height interval, from the ground to 15 km a.g.l., as a function of the time period between GC and
 550 launch; from left to the right, the time period increases from 1 to more than 5 days. In brackets within the legend, the
 551 number of parallel soundings considered for each time period is reported.
 552

553 In Figure 10, another way to study GC data is presented for the Payerne station. In this case, the
 554 average difference and the standard deviation of temperature and relative humidity found during
 555 the GC using Vaisala RS41 radiosondes into the Vaisala AS15 versus the aging (up to 9 days into tray
 556 from the loading until launch) is shown. For both temperature and relative humidity, excluding only
 557 the launches which occurred within 24 hours of the radiosonde loading, the bias is negative and
 558 independent of any further aging. Until one day after loading the bias is stable close to zero and
 559 thereafter it increases to about -0.1 K and -0.1% over the following days. These results show how
 560 the use of ARLs also in remote places or where it is required to upload in advance a large number
 561 of radiosondes, to launch with a few days of delay, do not appreciably lead to changes in the Vaisala
 562 GC.

563



564

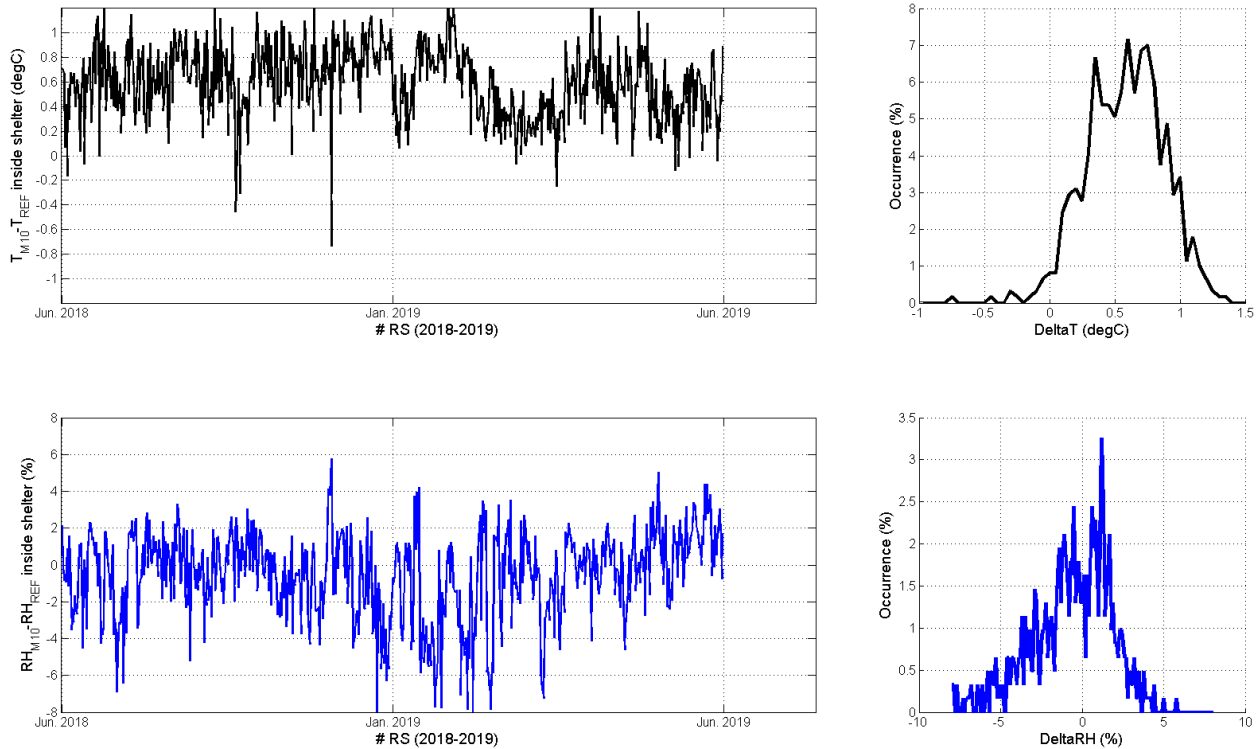
565 Figure 10: Average difference and standard deviation of temperature and relative humidity found during the Vaisala GC
 566 process versus the aging (number of days into tray from the loading until launch) of the radiosonde RS41 into the
 567 Payerne ARL (Vaisala AS15).

568

569 4.2. Performance of the Meteomodem ARL

570 The performance of the Meteomodem ARL ground-check has been evaluated through the analysis
 571 of a dataset collected at MétéoFrance Trappes station, where M10 radiosondes have been launched
 572 regularly at 11:30 and 23:30 UTC since 2016. The availability of a long time series for the comparison
 573 between M10 temperature and humidity sensor and a reference temperature/humidity sensor
 574 (Vaisala HMP110, https://www.vaisala.com/sites/default/files/documents/HMP110-Datasheet-B210852EN_1.pdf) at ambient conditions, inside a meteorological shelter for the Trappes station,
 575 permits the investigation of the system performance also in the pre-launch phase. Since June 2018,
 576 this comparison is carried out during the 5 minutes before each automatic sounding. Figure 11
 577 summarizes the time series and PDF of the difference between M10 and HMP110 sensor for
 578 temperature (black curve, upper panel) and relative humidity (blue curve, lower panel) recorded
 579 between June 2018 and June 2019. The relative humidity difference oscillates around 0% and in
 580 more than 75% of the cases the difference is smaller than 2% RH in absolute value. For temperature,
 581 the observed residual difference around 0.5°C requires further investigations.

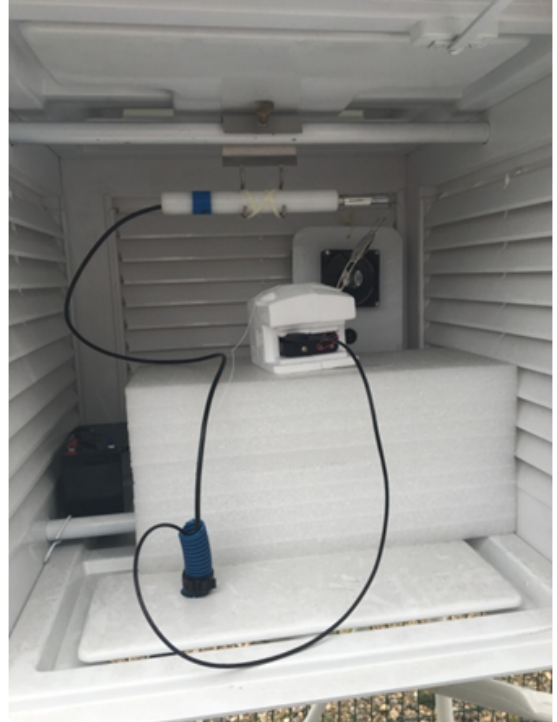
583



584

585 Figure 11: Time series and pdf of the difference between M10 and HMP110 sensor for temperature (black curve) and
 586 relative humidity (blue curve) between June 2018 and June 2019, measured at ground level inside a meteorological
 587 shelter in ambient condition.
 588

589 Figure 12 provides a picture of the meteorological shelter and the position of the HMP110 and the
 590 M10 during the 5-minutes comparison shown in Figure 11. These results need further investigations
 591 in order to determine if the systematic difference observed on temperature in the meteorological
 592 shelter is due to the Meteomodem M10 batches produced in 2018, though Meteomodem did not
 593 report similar systematic differences during the production checks, or if this could be due to the
 594 need for improvements in the experimental protocol. The meteorological shelter has been
 595 improved with the installation of a fan (Figure 12) which should produce a better homogenisation
 596 of the temperature and relative humidity around the two sensors. The development of a new
 597 experimental protocol is under consideration and should lead to the production of a tube ventilated
 598 by a laminar flow in which the Meteomodem M10 and a PTU reference could measure under the
 599 same environment, elucidating further upon the characterization of the spatial homogeneity of the
 600 temperature and relative humidity.
 601



602

603 Figure 12: Picture of the meteorological shelter in Trappes (left panel: general view: the meteorological is near the
604 Meteomodem ARL entrance for simplicity reasons, right panel: inside of the meteorological shelter)

605

606 Finally, the M10 radiosonde is put inside a SHC chamber for 3 minutes before the sounding (with a
607 relative humidity near 100%): more than 95% of the samplings are accepted after the test. For
608 operational reasons, the Meteomodem probes used in the GRUAN protocol are tested in the
609 meteorological shelter and in the 100% RH test but not necessarily in this order each time. It is not
610 known if the order of the checks makes any difference.

611

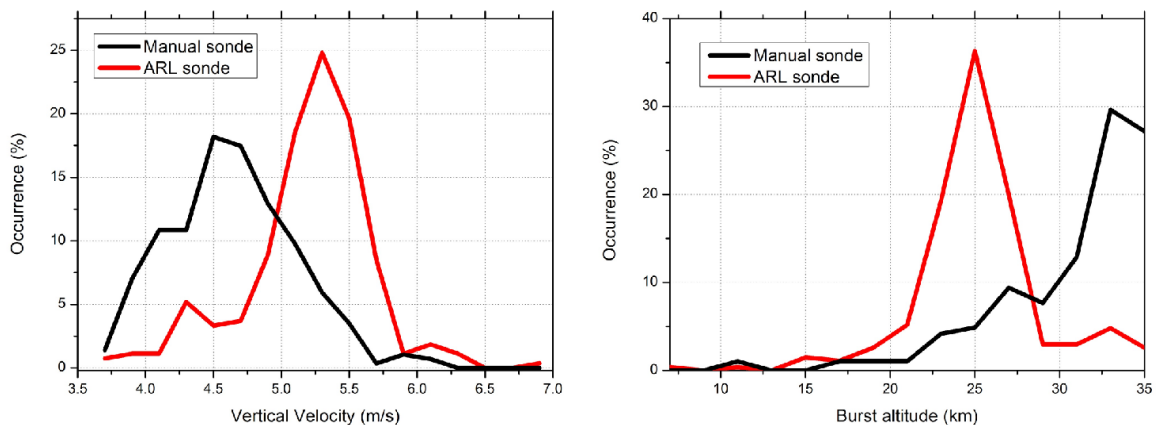
612 5. Vertical velocity and balloon burst

613 This section reports the statistics for the vertical velocity and the balloon burst altitudes from the
614 datasets collected at Sodankylä and Trappes stations.

615 5.1 Vertical velocity and balloon burst altitude for Vaisala technology

616 In Figure 13, the statistics of the balloon vertical velocity and of the burst altitude for Sodankylä in
617 the period from 2006 to 2012 are shown. In terms of vertical velocity (Figure 13, left panel), the ARL
618 has a quasi-symmetric frequency distribution peaked around 5.3 m s^{-1} with a spread mainly between
619 4.7 m s^{-1} and 5.9 m s^{-1} . For the manual launches, the frequency distribution is quite wide, non-
620 symmetric, peaked around 4.5 m s^{-1} with a larger spread of the values mainly between 3.5 m s^{-1} and
621 5.7 m s^{-1} . The comparison reveals the higher stability of the ARL compared to manual launches in

622 controlling the balloon filling and, therefore, the sounding vertical velocity which is relevant for the
 623 quality of the measured profile. For the balloon burst altitude (Figure 13, right panel), a like-for-like
 624 comparison between the manual launches and the ARL is not feasible at Sodankylä due to the use
 625 of different balloon types (typically smaller for the ARL) which causes a strong difference in balloon
 626 altitude. Totex Tx800 or Tx600 type of balloons were used in winter and Totex Ta350 or Tx350 type
 627 sounding balloons were flown during all other seasons. Due to smaller balloon volume, the
 628 summertime soundings had lower burst heights on average. The burst altitude for the ARL has also
 629 in this case a quasi-symmetric frequency distribution peaked around 25 km of altitude a.g.l with a
 630 spread of the values mainly between 17 km and 28 km a.g.l., while the distribution for manual
 631 launches is non-symmetric, with a maximum frequency around 33 km and most of values ranging
 632 within 21 - 35 km a.g.l. Differences between night-time and day-time soundings were not significant,
 633 although night time soundings have on average lower burst heights during polar vortex overhead
 634 conditions in winter.
 635



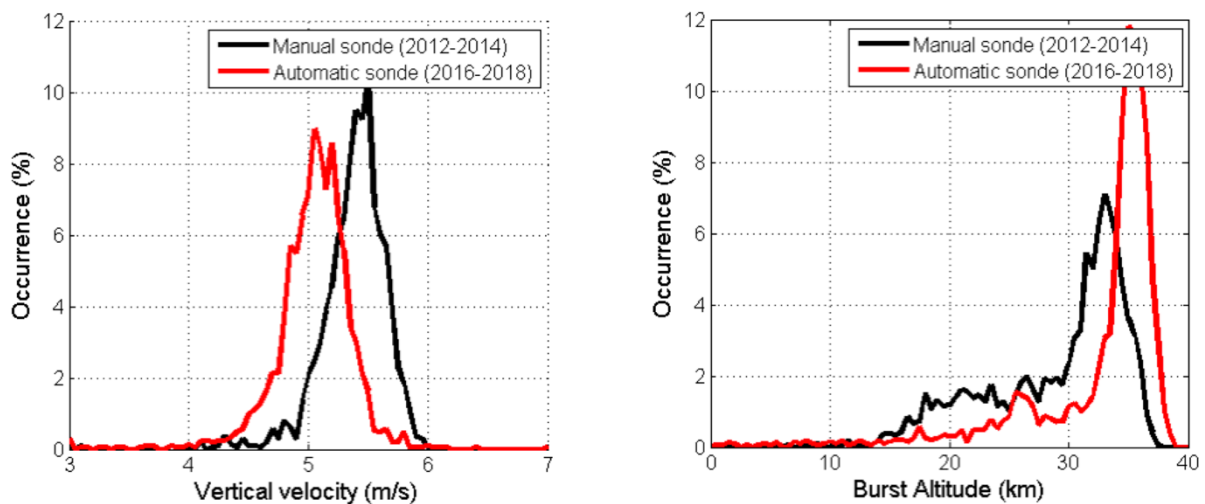
636
 637
 638 Figure 13: Vertical velocity (left panel) for radiosondes launched manually (black line) and automatically (red line), along
 639 with burst altitude (right panel) at Sodankylä station.
 640

641 5.2 Vertical velocity and balloon burst altitude for Meteomodem technology

642 A more interesting comparison to show the eventual positive influence of automation on the burst
 643 altitude is those related to the dataset discussed in Section 3 and summarized in Table 5, shared by
 644 Meteo France for Trappes station (Figure 14). In terms of vertical velocity (Figure 14, left panel),
 645 both the ARL and the manual launches have a quasi-symmetric frequency distribution peaked
 646 around 5.1 m s^{-1} and 5.5 m s^{-1} , respectively, with a similar spread of about 1.0 m s^{-1} . For the burst

647 altitude (Figure 14, right panel), we have for both the datasets a negatively skewed distribution with
 648 an evident peak around 33 km for the manual launches and 35 km for the ARL. The comparison
 649 reveals that the burst altitude (Figure 14, right panel) is generally higher for the ARL than for the
 650 manual launches, likely due to use of different balloons and the more limited human contact with
 651 the balloon which hence likely retains greater structural integrity. ARL frequency distribution has
 652 also a more peaked distribution that can be related to a more homogeneous balloon inflation
 653 (automatic inflation, same method, constant gas flow, more stable temperature). Furthermore, the
 654 vertical velocity of the balloon is stable (Figure 14, left panel). 40 % of the balloons burst before 30
 655 km during the manual period, where only 20 % do during the automatic period. This result means
 656 that the Meteomodem ARL and/or the operational procedures, elaborated under a joint effort by
 657 Meteomodem and MétéoFrance, has increased by a factor two the number of balloons reaching an
 658 altitude higher than 30 km. The burst altitude for both periods (2012-2014 for the manual launches
 659 and 2016-2018 for the ARL) shows some seasonal signal. It appears that burst altitude is lower
 660 during the winter. A further study could evaluate burst altitude as a function of air temperature or
 661 potential vorticity in order to study the influence of polar vortex and its potential impact on the
 662 burst altitude.

663
 664



665
 666
 667
 668
 669
 670
 671

Figure 14: Vertical velocity (left panel) for radiosondes launched manually (black line) and automatically (red line), along with burst altitude (right panel) at Trappes station.

672 **5.3 Quantifying relative performance**

673 In this section, two datasets are investigated to assess the differences in the vertical profiles of
674 temperature and humidity: the set of RS-92 parallel (automatic and manual) soundings performed
675 with the automatic radiosonde launchers at Sodankylä along with a second set of Meteomodem
676 radiosoundings collected at Faa'a station, French Polynesia. These are near-coincident launches but
677 the instruments are on physically distinct balloons which, as they ascend, likely at somewhat
678 different rates if the balloons are not filled identically, will follow subtly distinct pathways leading
679 to offsets in sampling. In the following analysis, given the latitude ϕ , the longitude λ , the Earth's
680 radius R (mean radius = 6371 km), the distance between two balloons (1 and 2) has been calculated
681 using the 'haversine' formula (Sheppard and Soule, 1922) which provides the great-circle distance
682 between two points (i.e., shortest distance over the earth's surface):

$$683 \quad d = Rc$$

684 where

$$685 \quad c = 2 \operatorname{atan2}(\sqrt{a}, \sqrt{(1-a)})$$

$$686 \quad a = \sin^2\left(\frac{\Delta\lambda}{2}\right) + \cos(\phi_1) \cos(\phi_2) \sin^2\left(\frac{\Delta\lambda}{2}\right)$$

687
688
689 The haversine formula remains particularly well-conditioned for numerical computation even at
690 small distances – unlike calculations based on the spherical law of cosines. The function “atan2” is
691 described in Glisson (2011).

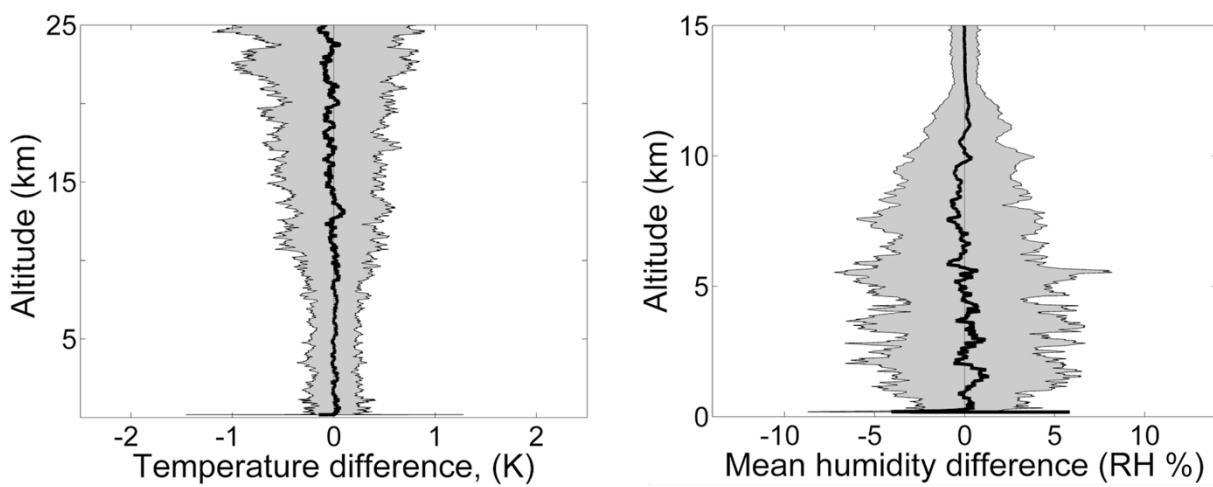
692 The two datasets are also investigated to show the correlation between the difference in the vertical
693 profiles and the distance between the two flying sondes.

694

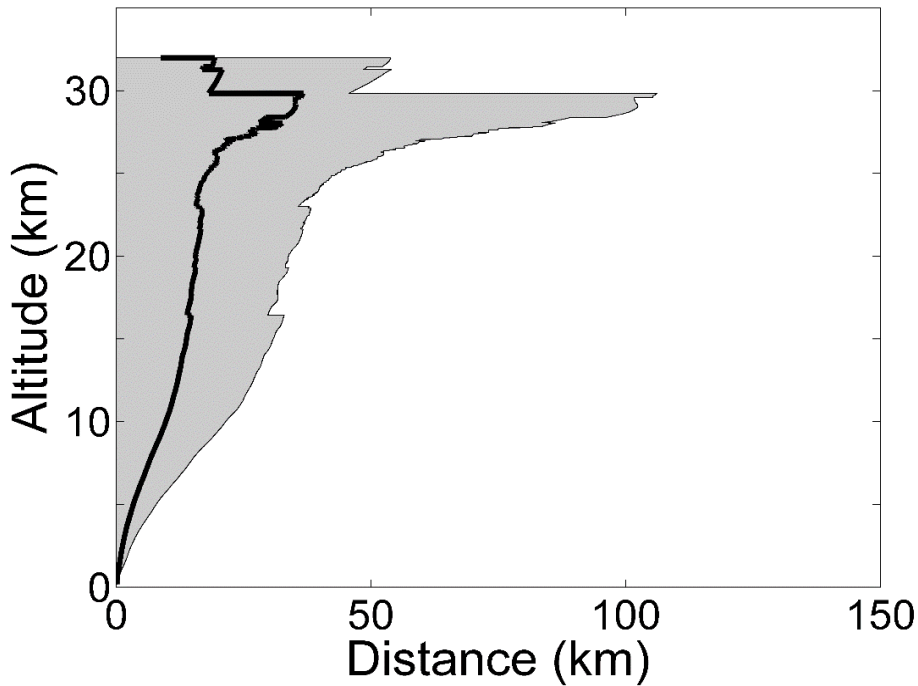
695 **5.4 Parallel soundings with Vaisala systems**

696 For the same six-year dataset collected at Sodankylä discussed in Section 4, the vertical profiles of
697 the average differences (automatic minus manual) and standard deviations of the temperature and
698 RH measured during parallel soundings are shown in Figure 15. Systematic differences in the
699 temperature profile are negligible (on average smaller than 0.01 K) over the entire vertical range up
700 to 25 km a.g.l, while the standard deviation increases with altitude from values smaller than ± 0.5 K
701 below 15 km to values larger than 1 K above. The result is in agreement with the increase in mean
702 distance between near simultaneous sonde paths at higher altitudes (Figure 16). A subset of the
703 parallel temperature soundings at Sodankylä has previously been analyzed by Sofieva et al. (2008).
704 Even though it is hard to separate difference components from non-colocation from those which

705 may arise from instrument-to-instrument differences (e.g. arising from manufacture variations and
706 differences in preparation, storage and launch at the uppermost altitudes), Sofieva et al. found
707 differences in small scale structures in temperature profiles, when the horizontal separation was
708 larger than 20 km. Moreover, to investigate whether the ARL and the manual radiosoundings
709 datasets were selected from populations having the same distribution, i.e. if the calculated mean
710 differences are statistically significant, the Wilcoxon Rank Sum test has been applied. The test result
711 confirms that the two datasets are samples of the same population showing a probability larger
712 than 0.5 for temperature at all the altitude levels below 20 km and larger than 0.1 above, while for
713 RH values the probability is larger than 0.3 over the entire range from the surface to 15 km a.g.l.



714
715 Figure 15: Temperature (left panel) and RH (right panel) mean difference between ARL and manual for the six-year
716 dataset of parallel soundings collected at Sodankylä station at all altitude levels up to 25 km a.g.l for temperature and
717 up to 15 km a.g.l for RH. Standard deviation at each pressure level is reported using the gray area.
718



719

720 Figure 16: Horizontal distance between the balloons calculated for the six-year dataset of parallel soundings collected
 721 at Sodankylä station for all the altitude levels up to 32 km a.g.l.

722

723 For the RH mean difference profile (Figure 15, right panel), there are no significant systematic
 724 differences up to 7 km and then again above 10 km a.g.l., while in between these altitudes a small
 725 negative mean difference lower than 1% RH is found and may be related to the RH variability in the
 726 upper troposphere and the increased distance between the two sondes. The increase in standard
 727 deviation in the lower troposphere below 5 km a.g.l., with values generally smaller than 5% RH, is
 728 due to the high RH variability which can be significant even for small horizontal distances between
 729 the two sondes. Above 5 km, and continuing through the profile to the UT/LS where the values of
 730 RH are on average smaller and less variable, RH difference decreases except when clouds or other
 731 uncommon events are detected (e.g. Stratospheric-Tropospheric exchanges).

732 In addition, the analysis was rerun after grouping the ARL flights according to the time a sonde had
 733 been loaded to the launcher system (see section 4): variations of time period between sonde loading
 734 and actual launch time did not influence the comparison results.

735 Finally, the Wilcoxon Rank Sum Test has been applied to the entire dataset and the computed
 736 probability that the two samples belong to the same population is larger than 0.35 at all altitude
 737 levels.

738

739

5.5 Parallel soundings at Faa'a with Meteomodem systems

740 A first evaluation of the performance of Meteomodem ARL is provided by the analysis of the
741 datasets collected over 3-14 October 2018 at Faa'a station (French Polynesia, station identifier=0-
742 20000-0-91938, 17.63S, 149.84W, 21 m a.s.l.) where 21 launches (9 day-time and 12 night-time) of
743 parallel radiosoundings have been undertaken (a picture is provided in Figure 17) in order both to
744 compare temperature, relative humidity, wind speed and direction, and to study further
745 characteristics of the flights (burst altitude, ascent speed for example). Meteo-France has
746 conducted the Intensive Operational Period while Institut Pierre Simon Laplace (IPSL) has produced
747 the NetCDF files (data and metadata) for the analysis. Raw data without any correction for
748 temperature and relative humidity have been considered in this paper. The GRUAN data processing,
749 which remains under development at the present time for this datastream, has not been applied.
750 The manufacturer Meteomodem IR2010 software was used for both manual and automatic
751 launches.
752



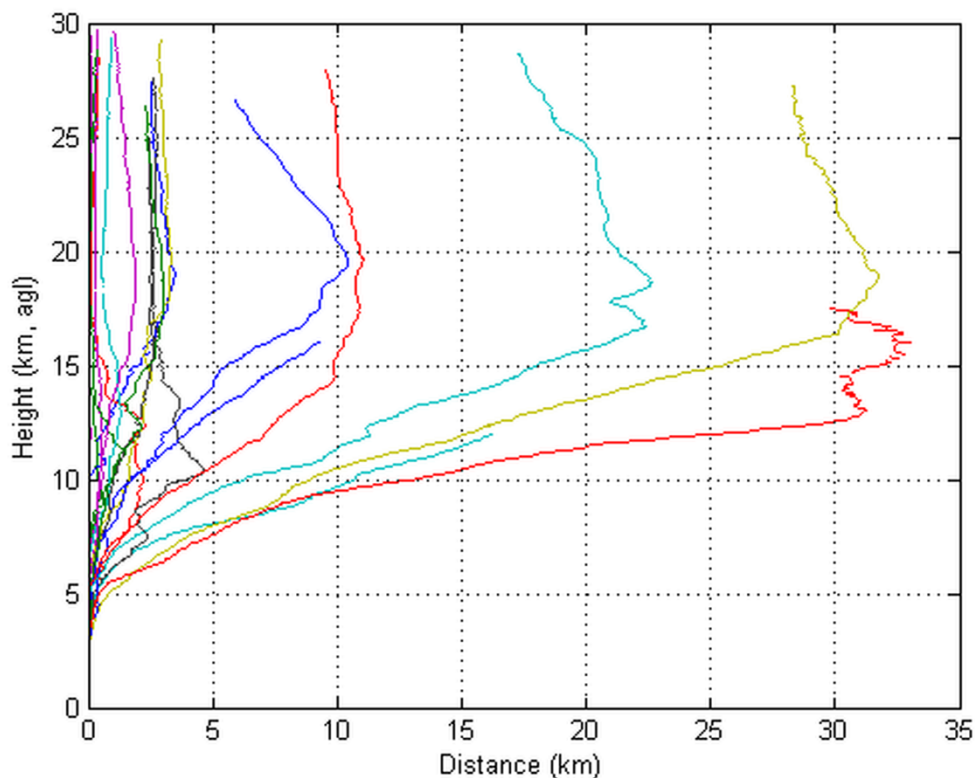
753
754 Figure 17: Daytime parallel sounding at Faa'a station (French Polynesia).
755

756 The dataset collected by Meteo-France at Faa'a station is not sufficiently large to draw robust
757 statistical inferences. Nevertheless, this dataset is the first ever available to evaluate the
758 performances of the Meteomodem ARL and can provide useful indications of any likely impact upon
759 the data quality of ARL facilities.

760 Before comparing, the T and RH profiles of the parallel sounding dataset have been interpolated to
761 a resolution of 100 m altitude. The difference between the launch time of the ARL and the manual
762 balloons ranges between 1 and 12 seconds.

763 In Figure 18, the horizontal distance between the pairs of parallel soundings at all the altitude levels
764 up to 25 km a.g.l. is shown: the horizontal distance between the two balloons is typically within
765 about 35 km.

766 In Figure 19, the mean difference between the set of ARL and manual parallel soundings profiles of
767 temperature and RH as a function of altitude regardless of time mismatch, along with the
768 corresponding standard deviation is shown. The left panel of Figure 19 shows the difference for
769 temperature, while the right panel shows it for RH. The mean temperature difference is smaller
770 than ± 0.2 K up to 12-13 km a.g.l., and typically smaller than ± 0.5 K above. The difference is negative,
771 up to -2.0 K, in the first 50-100 meters and this is probably due to the potential warming effect of
772 the ARL environment on the radiosonde sensor.

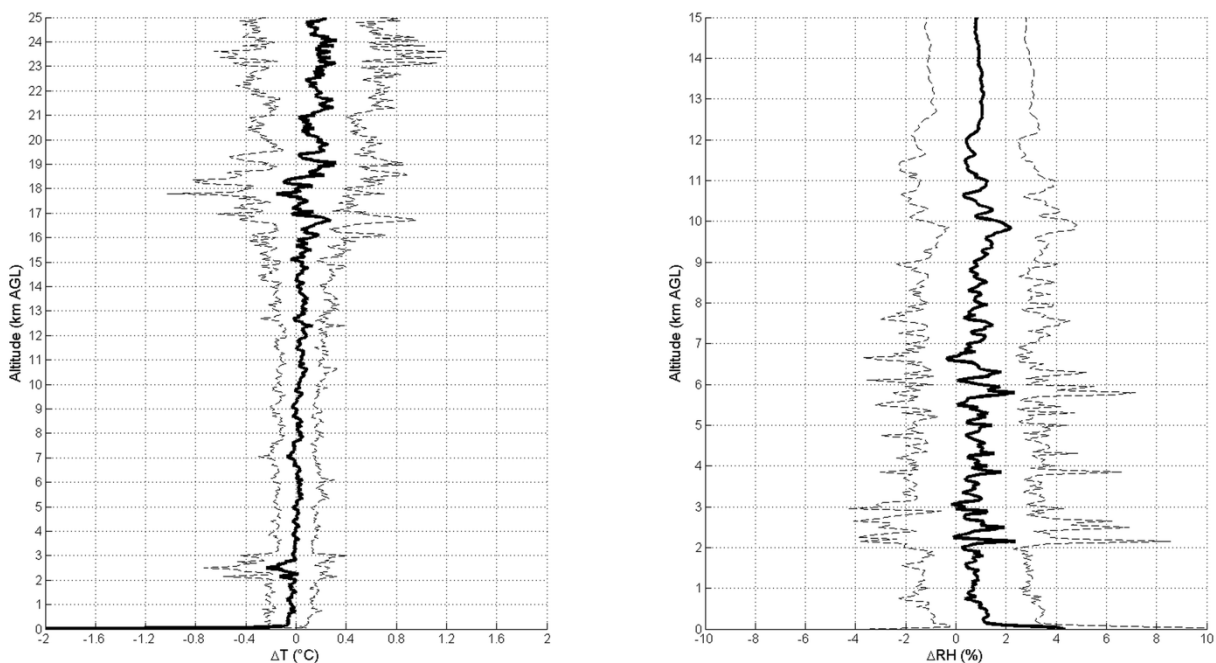


773
774 Figure 18: Horizontal distance calculated for the balloons of the 21 parallel soundings performed at Faa'a station for all
775 the altitude levels up to 25 km a.g.l. Measurement time between the two sondes at the same altitude levels may differ
776 and at the start time ranges within 1-12 seconds.
777

778 For RH, the mean difference is instead always positive and smaller than 0.7% RH up to 8 km a.g.l.
779 with a standard deviation smaller than 3-4% RH. Above 8 km, the mean difference becomes larger
780 and less variable with a maximum of about 2% RH and a standard deviation around 3%. The
781 Wilcoxon Rank rank sum test has been applied to both temperature and RH. For temperature, the
782 probability is higher than 0.3 until 17 km and higher than 0.2 above, while for RH is larger than 0.2

783 below 10 km and larger than 0.1 above. Only in the first 40 m for temperature and the first 20 m for
 784 RH, the Wilcoxon Rank rank sum test fails with a probability lower than 0.05. The results of the test
 785 confirm the null hypothesis of the same median for the ARL and manual data distribution at all the
 786 height levels for both temperature and RH, with the only exception of a few decameter above the
 787 ground because of the ARL air conditioned effect. The reason behind this bias could arise from GC
 788 effects or differences in the pre-launch procedures between the two systems affecting the
 789 performance of one of the two launches in a quasi-systematic manner throughout the vertical
 790 profile. This will be further investigated with the support of the manufacturer.

791 In terms of balloon burst altitude the ARL proved to be reliable both during the daytime with a burst
 792 altitude ranging within 26688 - 31904 m above ground level (a.g.l.) versus values within 24970 -
 793 30621 m a.g.l. calculated for the manual launches, while during nighttime the burst altitude ranges
 794 within 27587 - 30790 m a.g.l. for the automatic launcher versus values within 27437 - 30139 m a.g.l.
 795 for the manual launches. Applying the Wilcoxon Rank-Sum Test, the computed probability (0.05224)
 796 for the entire dataset is slightly greater than the 0.05 significance level and, therefore, the two
 797 distributions of burst altitudes are not significantly different indicating that ARL does not lead to
 798 significant improvements in the balloon burst altitude.



799 Figure 19: Difference between ARL and manual profiles of temperature (left panel) and RH (right panel) for 21 parallel
 800 soundings performed at Faa'a station up to 25 km a.g.l. for temperature and up to 15 km a.g.l. for relative humidity.
 801 Black lines: mean differences, dashed lines: standard deviation. A negative difference up to -2.0 K for temperature and
 802 smaller than smaller than 3-4% RH is observed in the first 50-100 meters probably due to the potential warming effect
 803 of the ARL environment on the radiosonde sensor.
 804
 805

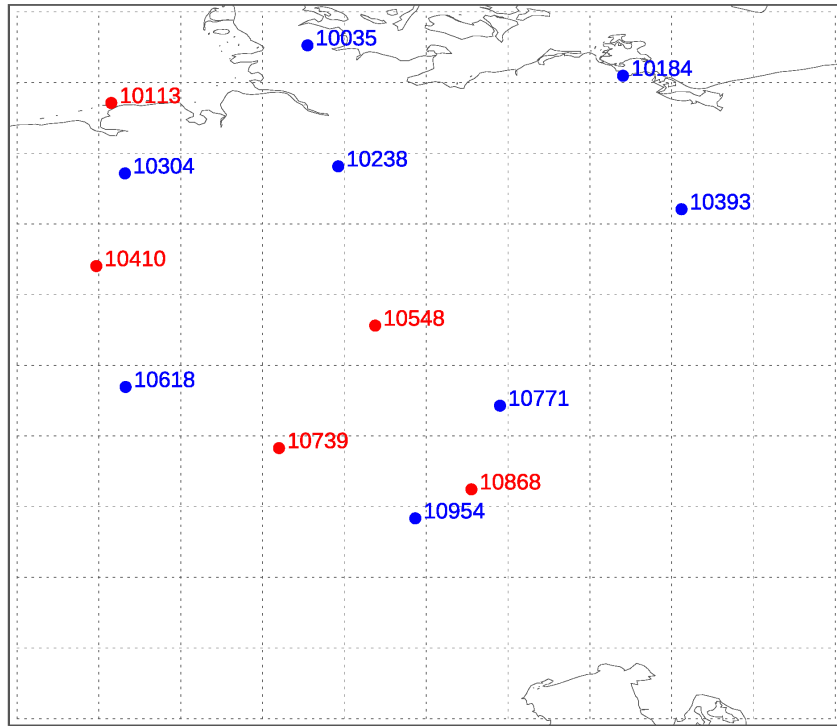
6. Automatic launchers performance evaluated using the ECMWF forecast model

806
807 Data assimilation systems compare observations with a short-range forecast (called the
808 background) and use observation-minus-background (O-B) differences in the assimilation to provide
809 improved initial conditions for the next forecast. For some areas/variables the uncertainties in the
810 background are now similar to, or smaller than, those in the observations, so the background
811 provides a very useful comparator. O-B differences from reanalyses have been also used to
812 homogenise historical radiosonde data (Haimberger et al., 2012). Ingleby (2017) compared different
813 radiosonde types with ECMWF background fields and for temperature and upper-tropospheric
814 humidity found differences in radiosonde performance that are broadly consistent with the results
815 of the last WMO radiosonde intercomparison (Nash et al., 2011) and are dominated by the sonde
816 type.

817 Statistics for Vaisala and Meteomodem radiosondes (manned and ARL) were produced. For Vaisala
818 we examined the German radiosondes (Figure 20) which form a relatively dense, well maintained
819 network with manned and ARL stations interspersed - ideal for this type of comparison. The
820 background uncertainties vary somewhat over time and regionally - they are probably slightly larger
821 over the UK because of the proximity of the North Atlantic. The Meteomodem samples were quite
822 small (from five French stations in total) and inconclusive; therefore, they will not be shown. No
823 attempts to provide a comparison of O-B statistics for Meisei ARL stations were carried out. This is
824 due to the fact that all four Meisei ARLs are on small islands, three to the south of the main islands
825 of Japan and one to the south-east, whereas the manned stations are on the main islands (or two
826 distant islands). Therefore, the O-B comparison could be affected by differences in the
827 background uncertainties over the southern islands relative to the main islands.

828 Figure 21 shows the numbers of reports at standard levels for German RS92 launches in the period
829 2017-2019 June. There are more than twice as many manned launches as ARL ascents because four
830 of the manned stations usually report four times per day whereas the other four manned stations
831 and the five ARL stations report twice a day. One interesting feature is that the proportion of ARL
832 ascents reaching 20 hPa is significantly higher than the proportion of manned ascents. A plausible
833 explanation for this is that ARLs put less stress on the neck of the balloon than manual launches
834 (Tim Oakley, pers. comm. 2018). During the middle months of 2017, there was a transition from
835 Vaisala RS92 to Vaisala RS41 at German stations - the proportions of RS41 reports at different
836 standard levels (not shown) are very similar to those in Figure 20.

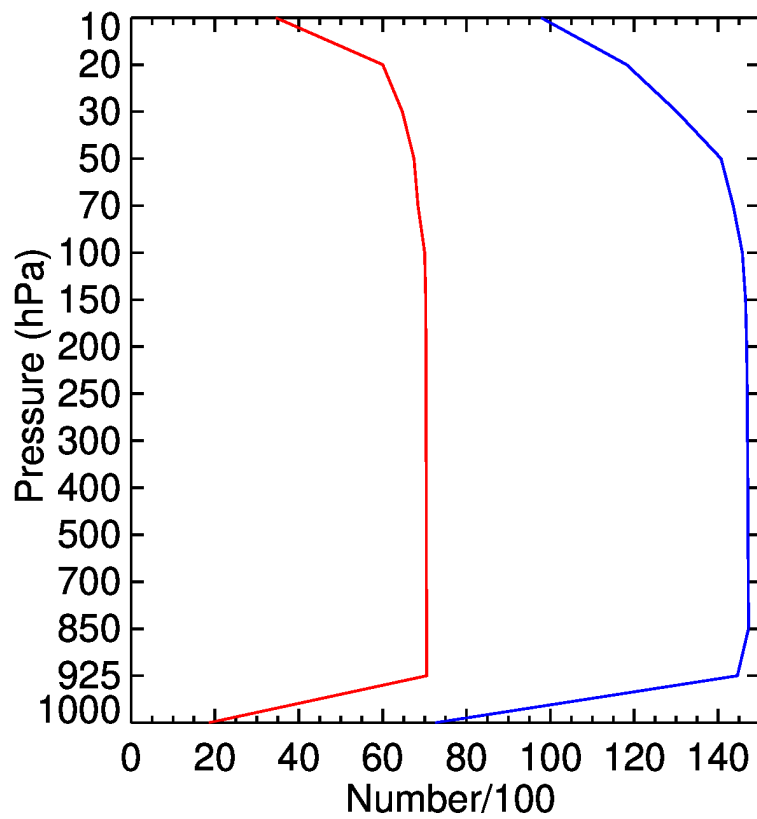
837



838

839 Figure 20: The main German radiosonde sites (two training/test sites not shown) and station identifiers: blue - manned
 840 stations (8), red - autosondes (5), as in early 2019 and for several years before that.

841



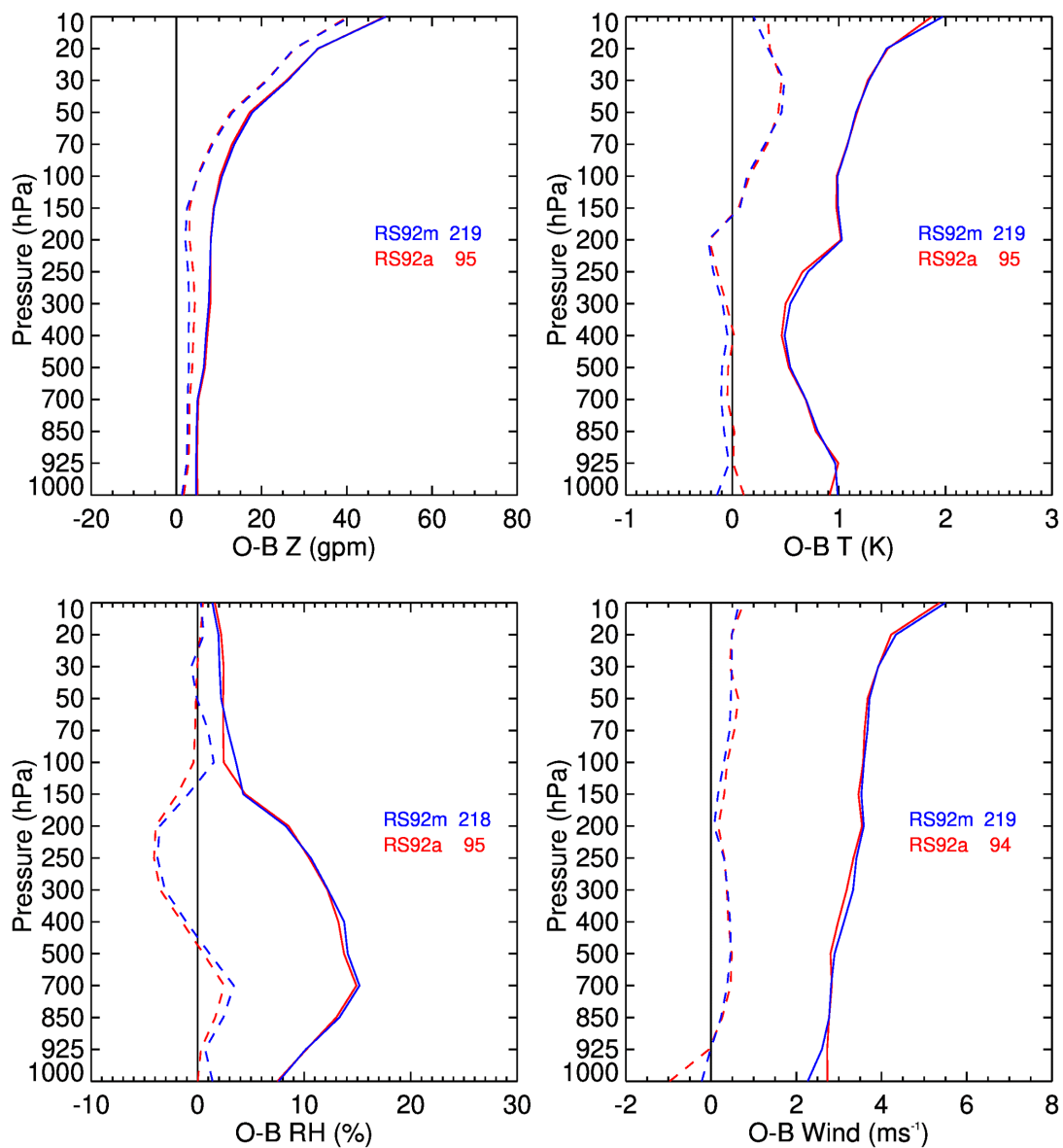
842

843 Figure 21. The number of temperature reports (hundreds) at standard levels, hPa, from German stations using Vaisala
 844 RS92 radiosondes, 2017-2019 June: blue - manned stations, red - autosondes. The numbers for other variables are very
 845 similar. There are fewer reports at 1000 hPa, and to some extent at 925 hPa, because these levels can be below the
 846 launch site. The decrease at upper levels is due to balloon burst.

847

848 Figures 22 and 23 compare O-B mean and root-mean-square (rms) statistics for German RS92 and
849 RS41 reports respectively (for technical reasons alphanumeric TEMP reports were used rather than
850 binary BUFR reports, see Ingleby and Edwards, 2014). The RS92 results (Figure 22) are very similar
851 between manned and ARL stations (small differences at 1000 hPa are presumably due to the
852 proximity of the surface and relatively small samples). The upper tropospheric humidity has minor
853 systematic differences probably due to humidity time-lag and radiation corrections being
854 introduced at different dates at different stations.

855



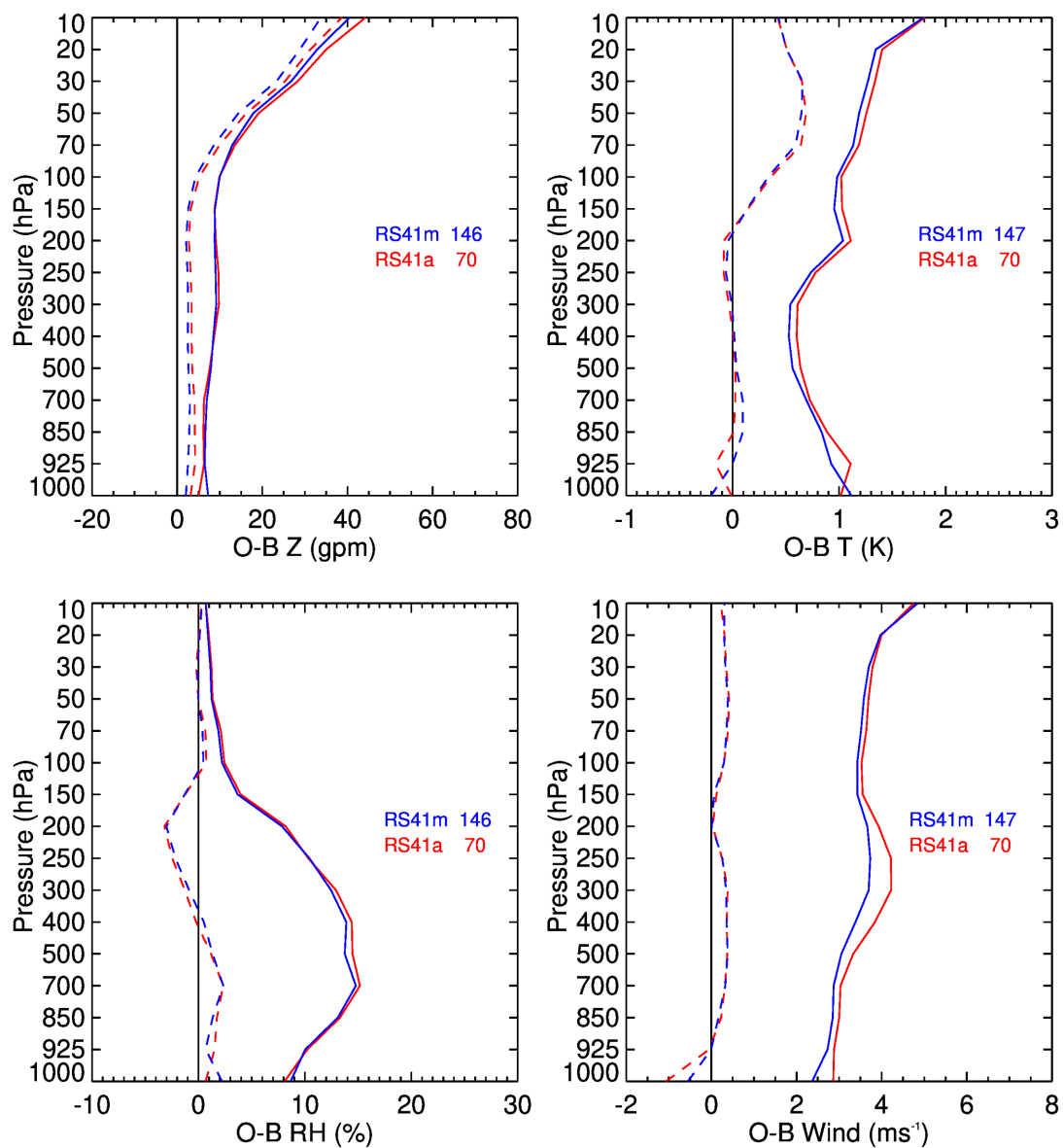
856

857 Figure 22: Mean (dashed) and rms (solid) O-B statistics for German RS92 ascents, 2015-2017: blue - manned, red - ARL.
858 Results for geopotential height (top left), temperature (top right), relative humidity (bottom left) and wind (mean wind
859 speed and rms vector wind; bottom right). The key gives the radiosonde code (RS92m for manual or RS92a for ARL) and
860 the number of reports in hundreds.

861

862 In contrast and surprisingly, the RS41 results (Figure 23) show rather larger rms(O-B) differences for
863 ARL stations - especially for temperature and wind. Qualitatively similar results for RS41 are found
864 for subsets of the period considered confirming the robustness of the results. The reasons for the
865 larger ARL rms differences in Figure 23 are not clear yet; one possibility is linked to the accuracy of
866 the reported pressure values. Pressure is measured by the RS92. For the RS41-SG the pressure is
867 calculated starting from a surface pressure measurement, but the German stations use the RS41-
868 SGP with a pressure sensor. Discussions with Vaisala and DWD (the German weather service) have
869 not so far revealed the cause.

870



871

872 Figure 23: As Figure 22 but for RS41 reports, 2017-June 2019. For some months, all stations reported as type 23 (123
873 in BUFR) so they had to be separated using the station identifiers.

874

875

876 **7. Summary and discussion**

877 In this paper, the existing Automatic Radiosonde Launchers available on the market (Vaisala,
878 Meteomodem and Meisei) are presented and a first comparative analysis of the performance,
879 relative to the more prevalent practice of manual launches, for the two most mature systems at
880 present (Vaisala and Meteomodem) has been reported. The analysis is limited to the data available
881 from a few GRUAN certified or candidate sites (Sodankylä , Payerne, Trappes, Potenza, Faa'a) and
882 to the investigation of the O-B bias and rms using the ECMWF forecast model and the Vaisala ARLs
883 and manual stations of the DWD. The data analysis allows us to infer the following principal
884 conclusions:

- 885 ● From a technical point of view, the performance of ARL is fully similar or superior to that
886 achieved with the traditional manual launches due to the capability of the automatic
887 launchers to fully control several parameters during the different phases of the radiosonde
888 preparation and balloon launch. This reduces launch-to-launch variability typical in manual
889 launches.
- 890 ● Despite having some potential advantages, there are still some issues generating failure in
891 the launches which can be improved according to the feedback provided by the GRUAN
892 sites, operating mainly Vaisala ARLs, such as the not infrequent failure of the power supply
893 system or of the air conditioning system, plenty of issues related to the balloon release in
894 the vessel area, likely contributing to early balloon bursts, and to the management of the
895 gas flow to fill the balloon, while the ready-to-launch sondes storage area appears to be the
896 most efficient part of ARLs.
- 897 ● For both temperature and relative humidity, the GC correction has been investigated for
898 the Vaisala ARL, finding a negative offset relative to manual launch procedures at different
899 stations and considering different radiosonde types (RS92/RS41) and batches of a few
900 tenths of degree and % RH, respectively. For the Meteomodem ARL at Trappes station, the
901 difference between M10 temperature and humidity sensor and the Vaisala HMP110 housed
902 in the ARL, used as a reference immediately prior to launch shows a few tenths of degree
903 and % RH, respectively. These results need further investigation to understand the
904 underlying reasons and whether manual or ARL operations are closer to the observed
905 atmospheric profiles.

- 906
- Systematic differences in the temperature profile for both Meteomodem and Vaisala are smaller than ± 0.2 K up to 10 hPa; RH profile differences are smaller than 1% RH for the Sodankylä Vaisala dataset up to 300 hPa, while it is constantly positive and smaller than 2% for Faa'a station Meteomodem series. However, the restricted dataset available at Faa'a station means caution should be applied in generalizing these results as representative of all Meteomodem ARL.
 - O-B mean and rms statistics for German RS92 and RS41 are very similar between manned and ARL stations. The upper tropospheric humidity has minor systematic differences probably due to humidity time-lag and radiation corrections being introduced at different dates at different stations. The RS41 sondes shows larger rms(O-B) differences for ARL stations than RS92, in particular for temperature and wind. The accuracy of the reported pressure values might be a possible reason to explain this difference.
- 918

919 As mentioned at the beginning of section 3, the factor limiting adoption of ARL radiosounding products within the GRUAN reference network is mainly related to the use of independent and traceable calibration standards like the Standard Humidity Chamber (SHC) within the ARLs. At present, for the different ARLs, this is possible but only before the sonde loading in the ARL trays. GRUAN Data Processing (GDP) is currently applied to the ARL soundings performed by the GRUAN stations though the related measurement programs cannot as yet be certified as GRUAN products. The present analysis has provided a substantive move forwards towards this aim by showing that performance is broadly comparable to manual launches.

927 In the last five years, several discussions within and outside the GRUAN community, involving also the manufactures, allowed to identify a few possibilities to meet the full traceability for the ARLs. Identified solutions to test are related to two main options:

- Use of a SHC (plus a reference thermometer, such as PT100 sonde) immediately after the manufacturer GC and prior to loading the sondes;
- Use of reference thermometer and hygrometer within the the ready-to-launch sondes storage area, as close as possible to the radiosonde sensors, with the optional use of a few additional thermometers and hygrometers within the storage area to monitor the uniformity of the temperature and relative humidity within the same area.

936 Both approaches have advantages and drawbacks. The first allows use of the SHC as a traceable calibration standard at or around 100 % relative humidity, depending on the solution used in the

938 SHC. Nevertheless, the proposed two stage procedure can be applied only in advance of the launch
939 and tests are needed to confirm what was already shown in Section 4 at Sodankylä and Payerne
940 stations, i.e. a sonde can be launched within a few days from its upload in the ARL without differing
941 significantly from the SHC collected data.

942 The second approach can instead continuously monitor the radiosonde during the entire launch
943 procedure in the storage area and before the sonde tray is moved out to the vessel area for launch,
944 when temperature and RH within the storage area may rapidly change because of the incoming air
945 from outside the vessel area. This approach cannot directly use traceable calibration standards but
946 it must be based on the comparison with reference thermometers and hygrometers calibrated on
947 a routine and certified basis. In addition, the sonde calibration cannot be monitored at 100 % RH
948 because the air conditioning system within the ARL keeps stable humidity conditions and cannot be
949 modified to avoid an impact on the ARL operation efficiency.

950 For both the approaches above, a customized solution to collect the data and use them in the
951 generation of a GDP must be found given the constraints of the ARL software which does not allow
952 extra calibration or comparison values to be collected or saved in the main radiosonde launch files.

953 It must be noted that at 4 JMA stations, not belonging to GRUAN, the Vaisala ARL is used adopting
954 a modified setup of the AS15 system including an additional GC based on reference instruments
955 developed by Vaisala for temperature and humidity, i.e Vaisala HMP155 with HMT333, lodged in a
956 custom-made chamber. When loading the radiosonde, the JMA specified GC for temperature and
957 humidity is also performed, in line with JMA's rule for upper air observations, specifying that the
958 PTU radiosonde sensors should be compared to reference sensors before launch only to confirm
959 that the difference is within a pre-defined threshold, while reference values are not used for any
960 correction of the measured profiles. The JMA additional GC is not a traceable calibration standard
961 and does not allow to perform the 0% RH and 100% RH ground calibration immediately before the
962 launch. Instead, it can be made when the radiosonde is uploaded in the ARL using a method to save
963 the measured comparison values.

964 More details on the JMA specified ground check for temperature and humidity are available at:
965 <https://www.vaisala.com/sites/default/files/documents/RI41-Datasheet-B211322EN.pdf>.

966 The compilation of the table of ARL systems in Appendix A (also the plot in Figure 1) brought home
967 that it is not easy for users to know which stations are using ARLs. We recommend that information
968 on automated launchers (type, start date, end date if appropriate) should be included in the
969 OSCAR/Surface catalogue.

970 Other issues which must be considered and solved to provide a GDP from ARLs are related to the
971 need to supply the manufacturer software with an accurate local pressure measurement and its
972 height at the launch time. Delays between the actual and the reported launch time from the
973 software is another issue which is under investigation by the GRUAN community.

974 The GRUAN community is discussing a strategy to achieve the full traceability for the ARL products
975 and to ascertain if any of the approaches described above can be tested intensively at one or more
976 sites: unfortunately, many of the GRUAN sites are also operational stations from the Met Services
977 and from other research institutions and are not readily available for testing. The next step will be
978 to identify which sites can perform specific tests on the ARL traceability and to collect as many
979 metadata as possible from all the GRUAN sites to report, in following publications, extensive
980 statistics validating the results presented in this paper.

981

982 **8. Author contribution**

983 Fabio Madonna with the help of Rigel Kivi and Masatomo Fujiwara worked on the paper
984 conceptualization and on the methodology. Fabio Madonna, Rigel Kivi, Jean-Charles Dupont, Bruce
985 Ingleby, Gonzague Romanens, Miguel Hernandez, Masami Iwabuchi, Shunsuke Hoshino and Peter
986 Thorne have been involved in the formal analysis. All the co-authors contributed to the writing of
987 original draft, review and editing.

988

989 **9. Competing interests**

990 The authors declare that they have no conflict of interest.

991

992 **10. Acknowledgements**

993 Much useful information has been provided by the three manufacturers: Vaisala, Meteomodem and
994 Meisei. Information on which stations use Meteomodem ARLs was provided by Adrien Ferreira of
995 Meteomodem in April 2019. Hannu Jauhainen of Vaisala provided a list of stations using their
996 Autosonde including several which were not known from the WIS reports. MeteoFrance and several
997 other National Meteorological Services have also provided information. The Faa'a data discussed in
998 this manuscript are available at ftp://ftp.lmd.polytechnique.fr/jcdupont/data_m10_gruan_faa and
999 can be used or cited under the DOI number <https://doi.org/10.14768/20181213001.1>.

1000

1001 **11. References**

1002 Bodeker, G. E., Bojinski, S., Cimini, D., Dirksen, R., Haeffelin, M., Hannigan, J. W., Hurst, D. F., Leblanc,
1003 T., Madonna, F., Maturilli, M., Mikalsen, A., Philipona, R., Reale, T., Seidel, D., Tan, D., Thorne, P.,
1004 Vömel, H. and Wang, J.: Reference upper-air observations for climate: From concept to reality,
1005 *Bulletin of the American Meteorological Society*, 97 (1), pp. 123-135. doi: 10.1175/BAMS-D-14-
1006 00072.1, 2016.
1007
1008 Carminati, F., Migliorini, S., Ingleby, B., Bell, W., Lawrence, H., Newman, S., Hocking, J., and Smith,
1009 A.: Using reference radiosondes to characterise NWP model uncertainty for improved satellite
1010 calibration and validation, *Atmos. Meas. Tech.*, 12, 83–106, [https://doi.org/10.5194/amt-12-83-](https://doi.org/10.5194/amt-12-83-2019)
1011 2019, 2019.
1012
1013 Dirksen, R. J., Sommer, M., Immler, F. J., Hurst, D. F., Kivi, R., and Vömel, H.: Reference quality upper-
1014 air measurements: GRUAN data processing for the Vaisala RS92 radiosonde, *Atmos. Meas. Tech.*, 7,
1015 4463-4490, <https://doi.org/10.5194/amt-7-4463-2014>, 2014.
1016
1017 Glisson, T. H.: *Introduction to Circuit Analysis and Design*, Springer Science & Business Media, Ed. 1,
1018 XV, 768, 10.1007/978-90-481-9443-8, 2011.
1019
1020 Haimberger, L., C. Tavorato, S. Sperka: Homogenization of the Global Radiosonde Temperature
1021 Dataset through Combined Comparison with Reanalysis Background Series and Neighboring
1022 Stations, *J. Clim.*, 25, 8108–8131, doi:10.1175/JCLI-D-11-00668.1, 2012.
1023
1024 Ho, S.-P., Peng, L., and Vömel, H.: Characterization of the long-term radiosonde temperature biases
1025 in the upper troposphere and lower stratosphere using COSMIC and Metop-A/GRAS data from 2006
1026 to 2014, *Atmos. Chem. Phys.*, 17, 4493-4511, <https://doi.org/10.5194/acp-17-4493-2017>, 2017.
1027
1028 Ingleby B, Edwards D.: Changes to radiosonde reports and their processing for numerical weather
1029 prediction, *Atmosph. Sci. Lett.*, 16: 44-49. doi: 10.1002/asl2.518, 2014
1030
1031 Ingleby, B.: An assessment of different radiosonde types 2015/2016. ECMWF Tech. Memo. 807, 69
1032 pp., [https://www.ecmwf.int/sites/default/files/elibrary/2017/17551-assessment-different-](https://www.ecmwf.int/sites/default/files/elibrary/2017/17551-assessment-different-radiosonde-types-20152016.pdf)
1033 [radiosonde-types-20152016.pdf](https://www.ecmwf.int/sites/default/files/elibrary/2017/17551-assessment-different-radiosonde-types-20152016.pdf), 2017.
1034
1035 Kobayashi, E., Hoshino, S., Iwabuchi, M., Sugidachi, T., Shimizu, K., and Fujiwara, M.: Comparison of
1036 the GRUAN data products for Meisei RS-11G and Vaisala RS92-SGP radiosondes at Tateno (36.06° N,
1037 140.13° E), Japan, *Atmos. Meas. Tech.*, 12, 3039–3065, <https://doi.org/10.5194/amt-12-3039-2019>,
1038 2019.
1039
1040 Kostamo, P., *Advanced automation for upper-air stations*, WMO Instruments and Observing
1041 *Methods Report No. 49 (TECO-92)*, pp. 104-107.
1042 https://library.wmo.int/index.php?lvl=notice_display&id=11254#Xeo3GS2h01l, 1992
1043
1044 Lehtinen, R., T. Tikkanen, J. Räsänen, and M. Turunen: Factors contributing to RS41 GPS-based
1045 pressure and comparison with RS92 sensor-based pressure, WMO Technical Conference (TECO), St.
1046 Petersburg, Russia. [https://www.wmo.int/pages/prog/www/IMOP/publications/IOM-116_TECO-](https://www.wmo.int/pages/prog/www/IMOP/publications/IOM-116_TECO-2014/Session%201/P1_28_Lehtinen_RS41PressCompRS92.pdf)
1047 [2014/Session%201/P1_28_Lehtinen_RS41PressCompRS92.pdf](https://www.wmo.int/pages/prog/www/IMOP/publications/IOM-116_TECO-2014/Session%201/P1_28_Lehtinen_RS41PressCompRS92.pdf), 2014.
1048

1049 Lilja A., Franssila J., Hautaniemi P., Lehmuskero M. Review of the History and Future of Automatic
1050 Upper Air Soundings. TECO-2018, Amsterdam, the Netherlands. October 8th - 11th, 2018.
1051

1052 Madonna, F., Amodeo, A., Boselli, A., Cornacchia, C., Cuomo, V., D'Amico, G., Giunta, A., Mona, L.,
1053 and Pappalardo, G.: CIAO: the CNR-IMAA advanced observatory for atmospheric research, *Atmos.*
1054 *Meas. Tech.*, 4, 1191-1208, <https://doi.org/10.5194/amt-4-1191-2011>, 2011.
1055

1056 Madonna, F., Rosoldi, M., Güldner, J., Haefele, A., Kivi, R., Cadeddu, M. P., Sisterson, D., and
1057 Pappalardo, G.: Quantifying the value of redundant measurements at GCOS Reference Upper-Air
1058 Network sites, *Atmos. Meas. Tech.*, 7, 3813-3823, <https://doi.org/10.5194/amt-7-3813-2014>, 2014.
1059

1060 Nash J., T. Oakley, H. Vömel, and Wei Li.: WMO Intercomparison of High Quality Radiosonde
1061 Systems Yangjiang, China, 12 July - 3 August 2010, WMO Instruments and Observing Methods
1062 Report No. 107, 2011.
1063

1064 Sheppard, W. W., and C. C. Soule: Practical navigation, World Technical Institute, Jersey City, 1922.
1065

1066 Sherwood, S. C., C. L. Meyer, R. J. Allen, and H. A. Titchner: Robust tropospheric warming revealed
1067 by iterative homogenized radiosonde data, *J. Clim.*, 21, 5336–5352, doi:10.1175/2008JCL2320.1,
1068 2008.
1069

1070 Sofieva, V. F., F. Dalaudier, R. Kivi, and E. Kyrö: On the variability of temperature profiles in the
1071 stratosphere: Implications for validation, *Geophys. Res. Lett.*, 35, L23808,
1072 doi:10.1029/2008GL035539, 2008.
1073

1074 Thorne, P. W., D. E. Parker, S. F. B. Tett, P. D. Jones, M. McCarthy, H. Coleman, and P. Brohan:
1075 Revisiting radiosonde upper-air temperatures from 1958 to 2002. *J. Geophys. Res.*, 110, D18105,
1076 doi:10.1029/2004JD005753, 2005.
1077

1078 Vaisala: Vaisala Radiosonde RS41 Measurement Performance White Paper. Ref. B211356EN-A ©
1079 Vaisala, 2013.
1080

1081 Vaisala: Comparison of Vaisala Radiosondes RS41 and RS92 White Paper. Ref. B211317EN – B ©
1082 Vaisala, Helsinki, Finland, 2014. Vaisala: Vaisala Radiosonde RS41 White Paper – Ground Check
1083 Device R141. Ref. B211539EN-A © Vaisala, 2015.
1084

1087 **12. APPENDIX A: Table of ARL systems operating around the world**

1088 Table A1: ARL stations shown in Figure 1. For each station, the WMO ID, which is also part of the WIGOS code
1089 (<https://oscar.wmo.int/surface>), the latitude, the longitude, the country and the period of installation is reported. For
1090 the approximate installation date (year or year-month), the metadata have been collected from different sources (IGRA,
1091 ECMWF, manufacturers, personal communication from scientists and instrument operators). If the last column is empty,
1092 no clear information on the installation period at that station are available. For Vaisala systems the "radiosonde type"
1093 in the reports should indicate if an ARL is being used, but it has been found that this is not always coded correctly. For

1094 Modem and Meisei systems there is no way for the current code formats to indicate that an ARL has been used. The
 1095 list is ordered according to the WMO ID.
 1096
 1097

WMO ID	Latitude	Longitude	Country	Installed
01001	70.940	-8.668	Norway	Meteomodem 2019-09
01010	69.315	16.131	Norway	Vaisala 2014
01241	63.705	9.612	Norway	Vaisala 2001
01415	58.874	5.665	Norway	Vaisala 2013
01492	59.943	10.719	Norway	Vaisala 1997
02185	65.543	22.115	Sweden	Vaisala 1996
02365	62.532	17.436	Sweden	Vaisala 1994
02527	57.657	12.291	Sweden	Vaisala 1994
02591	57.671	18.345	Sweden	Vaisala pre-1996
02836	67.366	26.631	Finland	Vaisala 2005-12
02963	60.815	23.499	Finland	Vaisala 1998
03238	55.019	-1.878	UK	Vaisala 1999
03354	53.006	-1.250	UK	Vaisala 1999
03882	50.891	0.317	UK	Vaisala 2001
03918	54.503	-6.343	UK	Vaisala 2002

03953	51.939	-10.241	Ireland	Meteomodem 2015
04018	63.975	-22.588	Iceland	Vaisala 2006
04360	65.611	-37.637	Greenland	Meteomodem 2012
06610	46.813	6.943	Switzerland	Vaisala 2018
07110	48.444	-4.412	France	Meteomodem 2016-04
07145	48.770	2.010	France	Meteomodem 2015-04
07510	44.831	-0.691	France	Meteomodem 2012-06
07645	43.856	4.407	France	Meteomodem 2011-11
07761	41.918	8.792	France	Meteomodem 2014-06
08190	41.384	2.118	Spain	Meteomodem 2012
08221	40.465	-3.589	Spain	Vaisala 2002
08392	39.606	2.707	Spain	Vaisala 2002
08383	37.278	-6.911	Spain	Vaisala 2018
08430	38.002	-1.171	Spain	Meteomodem 2015
10035	54.527	9.550	Germany	Vaisala 2019-10
10113	53.712	7.152	Germany	Vaisala 2011
10410	51.404	6.968	Germany	Vaisala 2012
10548	50.562	10.377	Germany	Vaisala 2011

10739	48.828	9.201	Germany	Vaisala 2012
10868	48.245	11.553	Germany	Vaisala 2013
11010	48.232	14.201	Austria	Vaisala 2016
11120	47.260	11.355	Austria	Vaisala 2015
11240	46.994	15.447	Austria	Vaisala 2015
13388	43.327	21.898	Serbia	Meteomodem 2015
14430	44.101	15.339	Croatia	Vaisala 1999
16113	44.539	7.613	Italy	Vaisala 1999
16144	44.654	11.623	Italy	Vaisala 1998
45004	22.312	114.173	Hong Kong	Vaisala 2003
47155	35.170	128.573	S Korea	Vaisala 2001
47418	42.953	144.438	Japan	Vaisala 2010-03
47600	37.391	136.895	Japan	Vaisala 2010-03
47678	33.122	139.779	Japan	Meisei (Vaisala from 2003-06 to 2010-03)
47741	35.458	133.066	Japan	Vaisala 2010-03
47778	33.45	135.757	Japan	Vaisala 2010-03
47909	28.393	129.552	Japan	Meisei 2007-03

47918	24.337	124.165	Japan	Meisei 2006-03
47945	25.829	131.229	Japan	Meisei (Vaisala from 2005-03 to 2017-03)
60018	28.318	-16.382	Spain	Vaisala 2001
60096	23.705	-15.930	Morocco	Meteomodem 2012
60155	33.559	-7.667	Morocco	Meteomodem 2014
61980	-20.9	55.500	La Reunion	Meteomodem 2018-04
70026	71.287	-156.763	USA, Alaska	Vaisala 2010
70133	66.885	-162.597	USA, Alaska	Vaisala 2019
70200	64.513	-165.443	USA, Alaska	Vaisala 2019
70219	60.780	-161.838	USA, Alaska	Vaisala 2018
70231	62.953	-155.603	USA, Alaska	Vaisala 2018
70261	64.814	-147.859	USA, Alaska	Vaisala 2018
70273	61.175	-149.993	USA, Alaska	Vaisala 2018
70308	57.167	-170.22	USA, Alaska	Vaisala 2018
70326	58.678	-156.647	USA, Alaska	Vaisala 2019

70350	57.750	-152.494	USA, Alaska	Vaisala 2015
70361	59.503	-139.66	USA, Alaska	Vaisala 2018
70398	55.043	-131.571	USA, Alaska	Vaisala 2018
71964	60.733	-135.097	Canada	Vaisala 1997
78897	16.260	-61.510	Gaudeloupe	Meteomodem 2015
81405	4.830	-52.370	French Guyana	Meteomodem 2012-09
89859	-74.624	164.232	Antarctic (S. Korea)	Vaisala 2014
91592	-22.27	166.450	New Caledonia	Meteomodem 2016-06
91938	-17.63	-149.84	Tahiti	Meteomodem 2018-10
94170	-12.678	141.921	Australia	Vaisala 1998
94302	-22.241	114.097	Australia	Vaisala 1997
94312	-20.373	118.632	Australia	Vaisala 1998
94332	-20.679	139.488	Australia	Vaisala 1998
94430	-26.613	118.536	Australia	Vaisala 1998
94510	-26.414	146.257	Australia	Vaisala 1998

94637	-30.784	121.454	Australia	Vaisala 2000
94653	-32.13	133.698	Australia	Vaisala 1999
94659	-31.156	136.805	Australia	Vaisala 2000
94711	-31.484	145.897	Australia	Vaisala 1997
94776	-32.793	151.836	Australia	Vaisala 2002
94821	-37.748	140.775	Australia	Vaisala 2010
94995	-31.542	159.077	Australia	Vaisala 2010
95527	-29.49	149.847	Australia	Vaisala 1999
96996	-12.189	96.834	Australia	Vaisala 1997

1098
1099
1100
1101
1102
1103
1104
1105
1106

Table A2: Additional ARL systems not transmitting data through the WIS in 2019 or used only for tests and short campaign (not shown in Figure 1). The ARL from 08160 was relocated to 08383.

Identifier	Latitude	Longitude	Country	Installed
POT (GRUAN)	40.600	15.725	Italy	Vaisala 2004
08160	41.660	-1.000	Spain	Vaisala 2005 to 2016
72402 (test)	37.930	-75.480	USA	Vaisala 2014 Meteomodem 2017
71461 (test)	55.810	-117.890	Canada	Vaisala 2016 Meteomodem 2017
10141 (test)	53.650	10.117	Germany	Vaisala 2016

1107